The Journal of Chemical Physics

Supramolecular copolymers predominated by alternating order: Theory and application

Cite as: J. Chem. Phys. **151**, 014902 (2019); https://doi.org/10.1063/1.5097577
Submitted: 26 March 2019 . Accepted: 03 June 2019 . Published Online: 03 July 2019

Reinier van Buel, Daniel Spitzer, Christian Marijan Berac, Paul van der Schoot, Pol Besenius, and Sara Jabbari-Farouji

The Journal of Chemical Physics ARTICLE scitation.org/journal/jcp

Supramolecular copolymers predominated by alternating order: Theory and application

Cite as: J. Chem. Phys. 151, 014902 (2019); doi: 10.1063/1.5097577
Submitted: 26 March 2019 • Accepted: 3 June 2019 •
Published Online: 3 July 2019

Reinier van Buel,[1,2] Daniel Spitzer,[3] Christian Marijan Berac,[3,4] Paul van der Schoot,[2,5] Pol Besenius,[3,4] and Sara Jabbari-Farouji[1,a)]

AFFILIATIONS

[1] Institute of Physics, Johannes Gutenberg-University, Staudingerweg 7-9, 55128 Mainz, Germany
[2] Theory of Polymer and Soft Matter Group, Department of Applied Physics, Eindhoven University of Technology, P.O. Box 513, 5600 MB Eindhoven, The Netherlands
[3] Institute of Organic Chemistry, Johannes Gutenberg-University Mainz, Duesbergweg 10-14, 55128 Mainz, Germany
[4] Graduate School of Materials Science in Mainz, Staudingerweg 9, 55128 Mainz, Germany
[5] Institute for Theoretical Physics, Utrecht University, Princetonplein 5, 3584 CC Utrecht, The Netherlands

[a)] **Electronic mail:** sjabbari@uni-mainz.de

ABSTRACT

We investigate the copolymerization behavior of a two-component system into quasilinear self-assemblies under conditions that interspecies binding is favored over identical species binding. The theoretical framework is based on a coarse-grained self-assembled Ising model with nearest neighbor interactions. In Ising language, such conditions correspond to the antiferromagnetic case giving rise to copolymers with predominantly alternating configurations. In the strong coupling limit, we show that the maximum fraction of polymerized material and the average length of strictly alternating copolymers depend on the stoichiometric ratio and the activation free energy of the more abundant species. They are substantially reduced when the stoichiometric ratio noticeably differs from unity. Moreover, for stoichiometric ratios close to unity, the copolymerization critical concentration is remarkably lower than the homopolymerization critical concentration of either species. We further analyze the polymerization behavior for a finite and negative coupling constant and characterize the composition of supramolecular copolymers. Our theoretical insights rationalize experimental results of supramolecular polymerization of oppositely charged monomeric species in aqueous solutions.

I. INTRODUCTION

Biomolecular structures are typically formed of small building blocks that self-assemble into very complex and often symmetrical architectures.[1–5] These building blocks have a configurational functionality that allows for specific interactions between them. Their self-assembly thus leads to a high degree of control over the geometry of the assembled structures, which is critical for their functionality. For instance, the conformation of a protein and its biological functions are intrinsically linked.[4–7] Further examples of self-assembled structures in nature are phospholipid membranes, nucleic acid helices, and ribosomes.[3,8] In order to develop supramolecular polymers, a reversible self-assembly approach has been employed. In this method, the monomeric building blocks assemble through weak noncovalent bonds, i.e., interactions on the order of the thermal energy,[9–12] to yield larger polymeric structures. Typical supramolecular interactions are reversible coordination bonds, hydrogen bonds, electrostatic interactions, π–π stacking, and van der Waals interactions.[5,13–17]

Among naturally occurring self-assemblies, virus particles are prominent examples that have served as a source of inspiration for biomimetic supramolecular polymerization. A large part of the self-assembly into supramolecular structures and genome packaging into protective capsids is driven by electrostatic contributions.[8,14,18–21] A viromimetic self-assembly strategy has further been applied to develop candidates for drug delivery vehicles, optoelectronic devices, sensors, and medical diagnostics.[22] The self-assembly of monomeric building blocks through electrostatic interactions is

thus a powerful tool to create new nanostructured materials with tunable functionalities such as optical, electrical, or magnetic properties.[23] For example, Tomba *et al.*[24] used electrostatic interactions to create self-assembled supramolecular structures of rubrene on a gold substrate. They were able to show that a combination of long range electrostatic repulsion and short-range attractive interactions drives the self-assembly into characteristic 1D patterns.

Recently, some of us[25,26] have developed a strategy to construct supramolecular copolymers using positively and negatively charged monomeric building blocks with C_3 symmetry, containing three identical peptide arms. These arms contain amphiphilic oligopeptides, based on alternating sequences of hydrophobic phenylalanine or methionine and charged lysine or glutamic acid residues, and form rodlike assemblies via a combination of electrostatic interactions, hydrogen bonding, and hydrophobic shielding.[25] The self-assembly is regulated via tuning the pH of the aqueous solutions.[25,26] By changing the charged state of the monomeric building blocks, pH drives the self-assembly into homopolymers of a neutral monomer or into copolymers when both monomer species carry complementary charges. A schematic representation of the supramolecular copolymerization occurring at neutral pH ≈ 7 is presented in Fig. 1(a).

Most recently, Ahlers *et al.* performed a light scattering and electron microscopy investigation of the fidelity of the supramolecular copolymer formation.[27] The anionic and cationic peptide comonomers self-assemble into AB-type heterocopolymers, with a nanorodlike morphology and a thickness of 11 nm. At equal concentrations of the two species, the copolymer mean length was 66 nm at an overall monomer concentration of 5×10^{-5}M, equivalent to a volume fraction of $\Phi \sim 2 \times 10^{-4}$. On the other hand, excess in either of the monomer species up to 50 mol. % in the stoichiometric ratio at the same overall monomer concentration decreased the mean copolymer length to about 42–50 nm.[27] These findings prompted us to gain a microscopic insight into the thermodynamic effects that dictate the configuration and formation of the copolymers from a theoretical perspective. Since circular dichroism and fluorescence spectroscopy tools have so far not been able to directly determine the composition of the supramolecular copolymers (alternating, random, or blocky structures), we gain a deeper understanding of the morphology and optimal stoichiometric ratio for alternating copolymers using a two-component coarse-grained model.[28] We further aim to fit the average length of copolymers from titration experiments with our theoretical framework and extract parameters that have been inherently difficult to determine using experiments alone.

Coarse-grained models for the self-assembly of monodisperse systems[14,29–31] have played an essential role in rationalizing experimental data. These models successfully describe the equilibrium self-assembly behavior of quasilinear supramolecular homopolymers for the so-called isodesmic, activated, and autocatalytic assembly cases. There has been an increasing interest in a theoretical understanding of the self-assembly behavior in multicomponent systems, and self-assembly theories have been extended to supramolecular copolymers consisting of two or more chemically distinct monomer species to capture the physics of the system under consideration.[28,32–42] In particular, a general statistical-thermodynamical treatment of one-dimensional multicomponent self-assembly in solutions using transfer matrix and sequence generating function methods has been developed, which provides a link to experimental observable quantities.[43] The general insights obtained from these studies are that the self-assembly behavior and especially the critical concentration and critical temperature strongly depend on the relative abundance of the self-assembling components and their interaction strengths.[28,40–42] Regarding the two-component self-assembly experiments described above, the 1D self-assembly theory for bidisperse systems in Ref. 28 is more relevant since electrostatic interactions can be explicitly incorporated. It builds on a two-component self-assembled Ising model where the presence of two different species

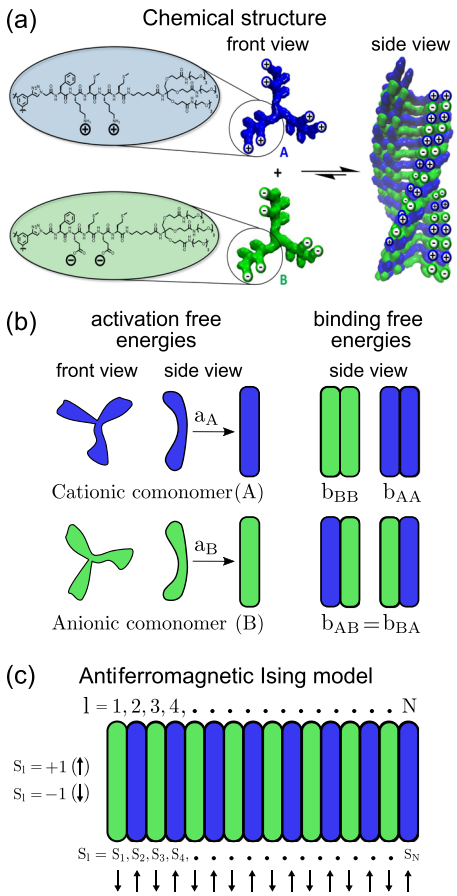

FIG. 1. (a) Chemical structures of the cationic dendritic peptide monomer (A, blue) and the anionic complementary monomer (B, green), and a schematic representation of the self-assembly into alternating supramolecular copolymers. (b) A schematic of the free energy parameters in our coarse-grained model. The activation free energies a_A and a_B are associated with the conformational changes of species A and B from the monomeric state to the self-assembled state, respectively. The binding free energy parameters b_{ij} account for the free energy gain of a monomer of species *i* binding to a monomer of species *j*. (c) A schematic representation of a copolymer of degree of polymerization *N*, which can be mapped to a 1D antiferromagnetic Ising model with nearest neighbor interactions described by a negative coupling constant given by $J \equiv (b_{AA} - 2\,b_{AB} + b_{BB})/4 < 0$. The spin at site $1 \le l \le N$ of the lattice S_l is 1 when the site is occupied by species *A* and −1 when occupied by species *B*.

is parameterized in terms of the strengths of binding free energies that depend on the monomer species involved in the pairing interaction. The theory predicts the formation of different morphologies of copolymer assemblies depending on the relative values of the species-dependent binding free energies, exhibiting random, blocky, and alternating ordering of the two components in the assemblies.

The decisive parameter determining the arrangement of monomer species in the assemblies (i.e., the morphology) is an effective *coupling constant* of the Ising model $J \equiv (b_{AA} - 2\,b_{AB} + b_{BB})/4$, which depends on a linear combination of the binding free energies b_{ij} between two monomer species $i, j \in \{A, B\}$. The $J > 0$ case, with favorable binding between monomers of the same species, leads to the formation of copolymers with blocky order. For the $J = 0$ case, monomers of the two species are randomly distributed along the assemblies, whereas the $J < 0$ case leads to copolymers with predominantly alternating order. The above mentioned model was thoroughly analyzed for the case of blocky ordering $J > 0$.[28] Here, we analyze the model for the $J < 0$ (antiferromagnetic coupling) case where the binding between two distinct species is favored over binding between those of the same type. We show that our model can rationalize the experimental results for the copolymerization of the two-component system with complementary charges, although it only incorporates nearest-neighbor interactions. This approximation works well because the long range electrostatic interactions of these 1D co-assemblies are effectively reduced to a nearest neighbor contribution due to *self-screening* effects in an alternating charge sequence.[44,45]

The remainder of this article is organized as follows. In Sec. II, we briefly review the theoretical framework of two-component supramolecular copolymers and discuss its main ingredients and the resulting mass-balance equations. In Sec. III, we analyze the mass-balance equations in the strongly negative coupling limit $J \ll -1$, where interspecies binding is predominant, and obtain the dependence of the critical concentration on the stoichiometric ratio and the free energy parameters. We investigate the copolymerization behavior for the case of finite and negative J in Sec. IV. Finally, we compare our theoretical insights to experimental findings in Sec. V and our main conclusions can be found in Sec. VI.

II. REVIEW OF THEORY OF SUPRAMOLECULAR COPOLYMERIZATION

In this section, we briefly review the supramolecular polymerization theory of linear assemblies for two-component systems developed in Ref. 28. We consider two monomeric species, A and B, with equal effective interaction volumes: $v_A = v_B = v$. The conformational free energy difference between a free monomer of type $i \in \{A, B\}$ in the solution and one bound to an assembly is parameterized by an activation free energy $a_i > 0$. The free energy gain of bonded interactions between two species i and j is parameterized by $-b_{ij}$, where $i, j \in \{A, B\}$. All the free energies are scaled to the thermal energy $k_BT \equiv 1$. See Fig. 1(b) for a schematic overview of the involved free energy parameters. The semigrand potential energy of a dilute solution of volume V containing free monomers and self-assembled polymers can be expressed by a sum of an ideal mixing entropy and contributions from the internal partition functions of assemblies with varying degrees of polymerization N,

$$\frac{\Omega}{V} = \sum_{N=1}^{\infty} \rho(N)[\ln \rho(N) v - 1 - \ln Z_N(\mu_i, b_{ij}, a_i)]. \tag{1}$$

Here, $\rho(N)$ is the number density of assemblies containing N monomers and μ_i represents the chemical potential of species $i \in \{A, B\}$. The semigrand canonical partition function $Z_N(\mu_i, b_{ij}, a_i)$ accounts for the Boltzmann weighted sum of all the conformational states of assemblies with size N.

Minimizing the grand potential energy $\delta\Omega/\delta\rho(N) = 0$ yields the equilibrium size distribution of assemblies,

$$\begin{aligned} \rho(1) v &= Z_1 = \mathrm{e}^{\mu_A + a_A} + \mathrm{e}^{\mu_B + a_B}, \\ \rho(N) v &= Z_N \qquad\qquad (N > 1). \end{aligned} \tag{2}$$

We note that our theory is formulated in such a way that the conformational free energy of an unbound monomer of species i is lower by an amount $-a_i$ relative to that of the bonded one. Therefore, the activation free energies a_i only enter in the single monomer partition function Z_1 and $Z_{N>1}$ does not depend on a_i explicitly as will be seen in the following. The partition function Z_N of assemblies in a two-component system can be obtained by mapping the Hamiltonian of linear assemblies onto an Ising model with an effective Hamiltonian of the form[28]

$$-\mathcal{H}_{N>1} = J \sum_{l=1}^{N-1} S_l S_{l+1} + H \sum_{l=1}^{N} S_l + E_0(N) - (S_1 + S_N)(b_{AA} - b_{BB})/4, \tag{3}$$

where $S_l = \pm 1$ is the spin state of the site l that is 1 when the site is occupied by species A and -1 when occupied by species B [Fig. 1(c)]. The effective coupling constant J between two neighboring sites is given by

$$J \equiv (b_{AA} - 2\,b_{AB} + b_{BB})/4, \tag{4}$$

and

$$H \equiv (b_{AA} - b_{BB} + \mu_A - \mu_B)/2 \tag{5}$$

describes the effective external field that couples to the spin sites. It is directly linked to the difference in the chemical potential of the two species $\Delta\mu \equiv (\mu_A - \mu_B)/2$. Furthermore, the spin-independent term

$$E_0(N) \equiv (N - 1)\,\bar{b} + N\,\bar{\mu} \tag{6}$$

defines the average binding free energy $\bar{b} = (b_{AA} + b_{BB} + 2b_{AB})/4$ and the average chemical potential $\bar{\mu} = (\mu_A + \mu_B)/2$ of the two-component system.

The coupling parameter J is the key quantity that determines the composition of monomers in the self-assembled polymers. For $J > 0$, ferromagnetic ordering is favored, implying blocky copolymers. $J = 0$ corresponds to paramagnetic ordering meaning random copolymers. The $J < 0$ case leads to antiferromagnetic ordering associated with alternating order in copolymers. It is of relevance to the experiments of oppositely charged monomers and will be thoroughly analyzed in the remainder of this article.

Using the standard transfer matrix method,[46] the partition function of an assembly of size $N > 1$ with open boundary conditions becomes[28]

$$Z_{N>1} = \left(x_+ \lambda_+^{N-1} + x_- \lambda_-^{N-1}\right) \exp E_0(N), \tag{7}$$

where the eigenvalues of the transfer matrix $\lambda_\pm$ are given by

$$\lambda_\pm = \mathbf{e}^{J}\cosh(H) \pm \mathbf{e}^{-J}\sqrt{\mathbf{e}^{4J}\sinh^2(H)+1}. \tag{8}$$

The coefficients $x_\pm$ are given by[28]

$$x_\pm = \cosh(\Delta\mu) \pm \frac{1+e^{2J}\sinh(\Delta\mu)\sinh(H)}{\sqrt{e^{4J}\sinh^2(H)+1}}, \tag{9}$$

describing the statistical weight associated with different possible configurations at the chain ends. They arise from the open boundary condition that implies either of species A or B can be located on either end of a chain.

To determine the values of the chemical potentials, we impose the mass conservation for the volume fraction of both species or alternatively for the overall volume fraction and the difference between the volume fraction of the two species. Here, we opt for the latter case. We denote the volume fraction of species i, monomers present in the solution either in the unbound or the self-assembled state, by Φ_i. The overall volume fraction of monomers $\Phi = \Phi_A + \Phi_B$ comprises the volume fractions of free monomers $\phi_i^{\mathrm{m}} = \mathbf{e}^{\mu_i + a_i}$ and all the bonded monomers in assemblies of varying sizes. The volume fraction of all the bonded monomers contributing to an assembly of size $N > 1$ can be obtained as $N\rho(N)v = NZ_N = \frac{\partial Z_N}{\partial \tilde{\mu}}$. Hence, the mass balance equation for the overall volume fraction of monomers reads

$$\Phi = \phi_A^{\mathrm{m}} + \phi_B^{\mathrm{m}} + \sum_{N=2}^{\infty} NZ_N. \tag{10}$$

This sum is easily evaluated using a geometric series, noting that the assembly partition function can be written as a sum of power laws

$$Z_{N>1} = \sum_{\sigma=\pm} x_\sigma \mathbf{e}^{\tilde{\mu}} \Lambda_\sigma^{N-1}, \tag{11}$$

where $\Lambda_\pm = \lambda_\pm \exp(\tilde{\mu}+\tilde{b})$ define effective fugacities of the bidisperse system. Noting that $\phi_A^{\mathrm{m}} + \phi_B^{\mathrm{m}} = Z_1$, the mass balance equation for the overall volume fraction can be written as

$$\Phi = \sum_{\sigma=\pm} \frac{x_\sigma \mathbf{e}^{\tilde{\mu}}}{(1-\Lambda_\sigma)^2} - (x_+ + x_-)\mathbf{e}^{\tilde{\mu}} + Z_1, \tag{12}$$

where $(x_+ + x_-)\mathbf{e}^{\tilde{\mu}} = \cosh(\Delta\mu)\mathbf{e}^{\tilde{\mu}} = \mathbf{e}^{\mu_A} + \mathbf{e}^{\mu_B}$. Similarly, the difference in the volume fraction of the two species $\Delta\Phi \equiv \Phi_A - \Phi_B$ includes the difference in the volume fraction of free monomers $\phi_A^{\mathrm{m}} - \phi_B^{\mathrm{m}}$ and the disparity in the number of A and B monomers within chains of size $N > 1$ given by $\frac{\partial Z_N}{\partial \Delta\mu}$. Therefore, it can be expressed as

$$\Delta\Phi = \phi_A^{\mathrm{m}} - \phi_B^{\mathrm{m}} + \sum_{N=2}^{\infty} \frac{\partial Z_N}{\partial \Delta\mu}. \tag{13}$$

Evaluating this sum with a geometric series yields

$$\sum_{N=2}^{\infty} \frac{\partial Z_N}{\partial \Delta\mu} = \sum_{\sigma=\pm} \frac{\Lambda_\sigma \mathbf{e}^{\tilde{\mu}}}{1-\Lambda_\sigma}\frac{\partial x_\sigma}{\partial \Delta\mu} + \frac{\mathbf{e}^{\tilde{\mu}} x_\sigma}{(1-\Lambda_\sigma)^2}\frac{\partial \Lambda_\sigma}{\partial \Delta\mu}. \tag{14}$$

Noting that $\partial/\partial\Delta\mu = \partial/\partial H$, the mass balance equation for the difference in the volume fractions reads

$$\Delta\Phi = \phi_A^{\mathrm{m}} - \phi_B^{\mathrm{m}} + \sum_{\sigma=\pm} \frac{\Lambda_\sigma \mathbf{e}^{\tilde{\mu}}}{1-\Lambda_\sigma}\frac{\partial x_\sigma}{\partial H} + \frac{\mathbf{e}^{\tilde{\mu}} x_\sigma}{(1-\Lambda_\sigma)^2}\frac{\partial \Lambda_\sigma}{\partial H}. \tag{15}$$

Simplifying the mass balance equations further yields

$$\Phi = \sum_{\sigma=\pm} \frac{x_\sigma \mathbf{e}^{\tilde{\mu}}}{(1-\Lambda_\sigma)^2} + \mathbf{e}^{\mu_A}(\mathbf{e}^{a_A}-1) + \mathbf{e}^{\mu_B}(\mathbf{e}^{a_B}-1), \tag{16}$$

$$\Delta\Phi = \mathbf{e}^{\mu_A}\mathbf{e}^{a_A} - \mathbf{e}^{\mu_B}\mathbf{e}^{a_B} + \sum_{\sigma=\pm} \frac{x_\sigma \mathbf{e}^{\tilde{\mu}}\Lambda_\sigma}{(1-\Lambda_\sigma)^2}\left[(1-\Lambda_\sigma)\frac{\partial \ln x_\sigma}{\partial H} + \frac{\partial \ln \lambda_\sigma}{\partial H}\right]. \tag{17}$$

The coupled sets of Eqs. (16) and (17) are the central equations that are solved throughout the rest of this paper to obtain the chemical potentials μ_i.

By determining the chemical potentials from the above set of equations, the mean degree of polymerization

$$\overline{N} \equiv \frac{\sum_{N=1}^{\infty} N\rho(N)}{\sum_{N=1}^{\infty}\rho(N)} = \frac{\Phi}{\sum_{N=1}^{\infty}\rho(N)v} \tag{18}$$

is straightforwardly evaluated because the sum in the denominator can be simplified to

$$\sum_{N=1}^{\infty}\rho(N)v = \sum_{\sigma=\pm}\frac{\mathbf{e}^{\tilde{\mu}}x_\sigma\Lambda_\sigma}{(1-\Lambda_\sigma)} + \mathbf{e}^{\mu_A+a_A} + \mathbf{e}^{\mu_B+a_B}. \tag{19}$$

Moreover, the fraction of polymerized material obeys the simple relation

$$f = 1 - \frac{\rho(1)v}{\Phi} = 1 - \frac{\mathbf{e}^{\mu_A+a_A} + \mathbf{e}^{\mu_B+a_B}}{\Phi}, \tag{20}$$

which is, in principle, an experimentally accessible quantity. As expected, in the limit of vanishing concentration of species j ($\mathbf{e}^{\mu_j} \to 0$), the theoretical model recovers all governing equations of a homopolymer system made of the other species $i \neq j$. In this limit, the effective fugacity obeys $\Lambda_+ = \exp(\mu_i + b_{ii})$ and the mass balance equation reduces to

$$\frac{\Phi}{\Phi^*} = \Lambda_+ + \mathbf{e}^{-a_i}\Lambda_+^2\frac{2-\Lambda_+}{(1-\Lambda_+)^2}, \tag{21}$$

in which $\Phi^* = \exp(a_i - b_{ii})$ is the so-called critical concentration.[47] It demarcates the transition from a monomer-dominated to a polymer-dominated regime.

The analytical solution of the coupled mass balance equations (16) and (17) is not generally known. However, for the special case of $b_{AA} = b_{BB}$, $a_A = a_B \equiv a$, and $\alpha = 1$, we can solve the mass-balance equations. In this case, Eq. (17) yields $\mu_A = \mu_B \equiv \mu$ and Eq. (16) becomes identical to the monodisperse mass balance equation [Eq. (21)], in which $\Lambda_+ \equiv 2\exp(\mu + b_{\mathrm{eff}})$ and $\Phi^* \equiv \exp(-b_{\mathrm{eff}} + a)$. Here, $b_{\mathrm{eff}} \equiv \tilde{b} + \ln[\cosh(J)]$ is an effective binding free energy that incorporates the effect of mixing of the two components in the assemblies. In the following, we analyze the copolymerization behavior for the case of a negative coupling constant $J < 0$.

III. STRONGLY NEGATIVE COUPLING LIMIT: STRICTLY ALTERNATING COPOLYMERS

In Sec. II, we gave a brief review of the self-assembly model for the two-component systems and its central equations. This model has been thoroughly analyzed for the case of positive coupling ($J > 0$),[28] which leads to copolymers with predominantly blocky order. In this paper, we focus on analyzing the model for a negative coupling constant ($J < 0$), which gives rise to copolymers with predominantly alternating order. In this section, we first examine self-assembly behavior in the strongly negative coupling limit $J \ll -1$. This limit corresponds to the situation that the free energy gain of interspecies binding is much greater than that of identical species binding, i.e., $b_{AB} \gg b_{AA}$ and $b_{AB} \gg b_{BB}$. We consider two distinct cases: (i) $b_{ii} \ll -1$, i.e., no binding takes place between identical species and $b_{AB} > 0$ can have any finite value, and (ii) $b_{AB} \gg 1$ and b_{ii} have finite values. As can be seen from Eq. (4), either of these conditions leads to $J \ll -1$ for which comonomers along the assemblies predominantly presume an alternating order. We first simplify the mass balance equations [Eqs. (16) and (17)] in the limit of $J \to -\infty$ and analyze the copolymerization behavior. Next, we inspect the dependence of the critical concentration on the stoichiometric ratio.

A. Mass balance equations

In the limit $e^J \ll 1$, the eigenvalues $\lambda_\pm$ in Eq. (8) simplify to

$$\lambda_\pm = \pm \mathbf{e}^{-J} + \cosh(H) e^J + \mathcal{O}(e^{2J}). \tag{22}$$

As a result, the effective fugacities reduce to

$$\Lambda_\pm = \pm \mathbf{e}^{\bar{\mu}+b_{AB}} + \mathbf{e}^{\bar{\mu}+(b_{AA}+b_{BB})/2} \cosh(H) + \mathcal{O}(e^{2J}). \tag{23}$$

This equation shows that in such a strongly negative coupling limit, the leading order term of the effective fugacities depends only on b_{AB} and $\bar{\mu}$. The second leading order term is independent of b_{AB} and only depends on b_{ii} and μ_i.

Likewise, Taylor expanding Eq. (9) up to the first order in e^J, the end cap weights $x_\pm$ in the strong coupling regime reduce to

$$x_\pm = \cosh(\Delta\mu) \pm 1 + \mathcal{O}(e^{2J}). \tag{24}$$

We note that in the strong coupling limit, the end cap weights are symmetric with respect to the particle species.

Keeping only the leading order terms, we obtain the N-dependent partition functions in the $J \to -\infty$ limit. They can be split into partition functions for assemblies with even and odd degrees of polymerization given by

$$Z_N^{\text{even}} = 2\exp[(N-1)b_{AB} + N\bar{\mu}](1 + \mathcal{O}(e^{2J})) = 2\exp[-\mathcal{H}_{AB}^{\text{even}}], \tag{25}$$

$$Z_{N>1}^{\text{odd}} = 2\cosh(\Delta\mu)\exp[(N-1)b_{AB} + N\bar{\mu}](1 + \mathcal{O}(e^{2J})) = \exp[-\mathcal{H}_{AB}^{\text{odd}}] + \exp[-\mathcal{H}_{BA}^{\text{odd}}]. \tag{26}$$

Here, $\mathcal{H}_{AB}^{\text{even}}$ is the free energy of an alternating copolymer consisting of $N/2$ units of AB or BA dimers. Likewise, $\mathcal{H}_{AB}^{\text{odd}}$ and $\mathcal{H}_{BA}^{\text{odd}}$ represent the free energies of alternating copolymers of the form $B(AB)_{(N-1)/2}$ and $A(BA)_{(N-1)/2}$, i.e., with an excess of B or A monomers, respectively. Thus, in the limit $J \to -\infty$, the partition functions only depend on b_{AB} and the chemical potentials and do not exhibit any singularity. In other words, in this limit, our results converge to that of a bidisperse system where only interspecies binding takes place, i.e., $b_{ii} \to -\infty$ and b_{AB} can have any arbitrary positive value. Notably, for the case of equal chemical potentials, the prefactor of the partition function for assemblies with an odd number of monomers, $\cosh(\Delta\mu)$, reaches its minimum value and $Z_N^{\text{even}} = Z_N^{\text{odd}}$. This implies that the free energy cost of adding another monomer to a polymer with an arbitrary size is $-(b_{AB} + \bar{\mu})$ and independent of N. For unequal chemical potentials, the fraction of alternating polymers with an even degree of polymerization is smaller than those with an odd degree of polymerization because the more abundant species, assuming to be B, can have a greater contribution to the polymerization by forming $B(AB)_{(N-1)/2}$ copolymers.

Using the leading order terms of Eqs. (22)–(24), the mass balance equation for the overall volume fraction of monomers, given by Eq. (16), simplifies to

$$\Phi = \frac{(\mathbf{e}^{\mu_A} + \mathbf{e}^{\mu_B})\left(1 + \Lambda_+^2\right) + 4\mathbf{e}^{-b_{AB}}\Lambda_+^2}{(1-\Lambda_+^2)^2} + \mathbf{e}^{\mu_A}(\mathbf{e}^{a_A} - 1) + \mathbf{e}^{\mu_B}(\mathbf{e}^{a_B} - 1), \tag{27}$$

in which $\Lambda_+ \equiv \exp(\bar{\mu} + b_{AB})$. Likewise, using $\partial/\partial H = \partial/\partial\Delta\mu$, Eq. (17) expressed in terms of the stoichiometric ratio $\alpha \equiv \Phi_A/\Phi_B$ simplifies to

$$\Phi\frac{\alpha - 1}{\alpha + 1} = \frac{(\mathbf{e}^{\mu_A} - \mathbf{e}^{\mu_B})\Lambda_+^2}{1 - \Lambda_+^2} + \mathbf{e}^{\mu_A + a_A} - \mathbf{e}^{\mu_B + a_B}. \tag{28}$$

The first term on the right hand side of the above equation arises from the asymmetry in the population of copolymers with odd degrees of polymerization. For stoichiometric ratios different from unity, odd-numbered copolymers that include a larger fraction of the more abundant species are preferred.

Even in the strong coupling limit, we cannot analytically solve this set of coupled equations for the chemical potentials. Only for the special case of equal concentration of the two species, $\alpha = 1$, and identical activation energies $a_A = a_B = a$, we can obtain an analytical solution for the mass balance equations. Under such conditions, Eq. (28) yields $\mu_A = \mu_B$, i.e., the concentration of free monomers of the two species is equal at any Φ. The mass balance equation for the overall concentration Eq. (27) simplifies to $\Phi = 2\mathbf{e}^{\mu_A}[(1-\Lambda_+)^{-2} + (\mathbf{e}^{a_A} - 1)]$. It can be expressed as a third order polynomial in terms of $\Lambda_+ \equiv \exp(\bar{\mu} + b_{AB})$ given by

$$\frac{\Phi}{\Phi_{AB}^*} = \Lambda_+ + \mathbf{e}^{-a}\Lambda_+^2\frac{2 - \Lambda_+}{(1-\Lambda_+)^2}, \tag{29}$$

where we have introduced the critical concentration $\Phi_{AB}^* \equiv 2\mathbf{e}^{-b_{AB}+a}$. Notably, this equation has exactly the same form as the mass balance equation of a monodisperse system given in Eq. (21). Therefore, alternating copolymers can be thought of as homopolymers composed of (AB)-dimer building units. An identical form for the mass balance equations in the two cases suggests that Φ_{AB}^* can be interpreted as the critical concentration of alternating copolymers. In Subsection III C, we obtain the dependence of the critical concentration on α for sufficiently negative J and show that Φ_{AB}^* is indeed the critical concentration for the $\alpha = 1$ case when $b_{ii} \to -\infty$. Before

that, we first investigate the solution of the simplified mass-balance equations.

B. Polymerization behavior

In this subsection, we analyze the polymerization behavior in the strongly negative coupling limit, $J \to -\infty$, for the case that $b_{AA} = b_{BB} \to -\infty$, leading to the formation of strictly alternating copolymers. As pointed out in Subsection III A, the mass balance equations in this limit do not exhibit any singularity and are valid for arbitrary values of b_{AB}. The only variables appearing in the resulting mass balance equations are the interspecies binding energy b_{AB} and activation free energies a_i. We fix the value of the binding free energy between the two comonomers to $b_{AB} = 14$. To reduce the number of parameters in the mass balance equations [Eqs. (27) and (28)], we assume equal activation free energies $a_A = a_B = a$. We investigate the polymerization behavior of copolymers with strictly alternating order as a function of the overall concentration and the stoichiometric ratio for different values of the activation free energy. We restrict our analysis to $0 < \alpha < 1$, as the results for the $\alpha > 1$ case can be obtained by an $\alpha \to 1/\alpha$ transformation.

Figures 2(a) and 2(b) show the fraction of polymerized material f as a function of the total volume fraction Φ at several values of the stoichiometric ratio for $a = 0$ and $a = 4$, respectively. In all the cases,

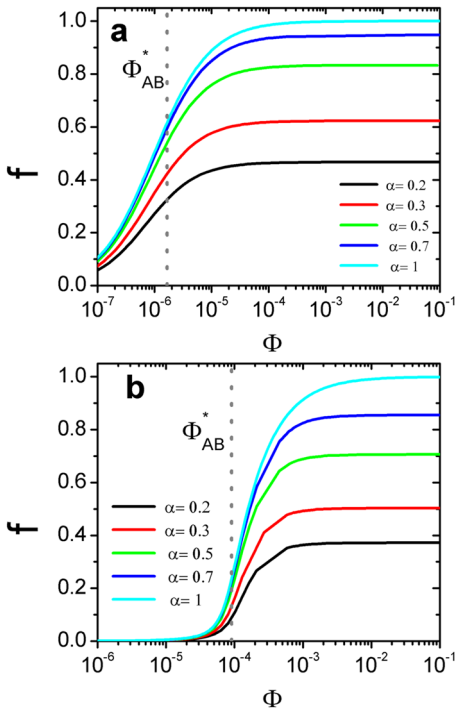

FIG. 2. Fraction of polymerized material f as a function of the overall volume fraction $\Phi = \Phi_A + \Phi_B$ at different stoichiometric ratios $\alpha = \Phi_A/\Phi_B$ in the limit of $J \to -\infty$ where no binding between identical species takes place, i.e., $b_{AA} = b_{BB} \to -\infty$. The assumed binding free energy between the two distinct species is $b_{AB} = b_{BA} = 14$, and the activation free energies in panels (a) and (b) are $a_A = a_B = 0$ and $a_A = a_B = 4$, respectively. The dotted lines show the critical concentrations $\Phi^*_{AB} = 1.66 \times 10^{-6}$ and $\Phi^*_{AB} = 9.08 \times 10^{-5}$ for $a = 0$ and $a = 4$, respectively.

we observe a transition from a monomer-dominated to a polymer-dominated regime for which the fraction of polymerized material reaches a maximum value, $f^{\max}$, that depends on the stoichiometric ratio and the activation free energy. Notably, $f^{\max}$ of copolymers with strictly alternating order is smaller than one except for the case of perfect stoichiometric balance $\alpha = 1$. $f^{\max}$ smaller than one reflects the lack of the less abundant species, i.e., type A monomers for the $\alpha < 1$ case. Copolymers with odd degrees of polymerization mainly exist in the $B(AB)_{(N-1)/2}$ form rather than the $A(BA)_{(N-1)/2}$ form to consume a larger amount of the B species. Similar to homopolymerization transition,[47] the sharpness of copolymerization transition depends on the strength of the activation free energy. It becomes steeper for larger activation free energies a. We can characterize the transition point as the monomeric volume fraction for which $f \approx 2/3 f^{\max}$. This value shifts to a higher value for the larger activation free energy, and it roughly agrees with the critical concentration value defined earlier as $\Phi^*_{AB} \equiv 2e^{-b_{AB}+a}$. The dotted lines in Figs. 2(a) and 2(b) correspond to $\Phi^*_{AB} = 1.66 \times 10^{-6}$ and $\Phi^*_{AB} = 9.08 \times 10^{-5}$ for $a = 0$ and $a = 4$, respectively.

At large Φ, in the saturation regime where most of the type A monomers are consumed, we expect $\mu_A \ll \mu_B$. We can use this approximation to solve the mass balance equations Eqs. (27) and (28) analytically and estimate the fraction of polymerized material as $f^{\max} \approx 1 - e^{\mu_B + a}/\Phi$. Doing so, we obtain the functional dependence of $f^{\max}$ on a and α as

$$f^{\max} = \frac{4\alpha(e^a - 1) + \sqrt{1 + 4(1-\alpha)\alpha(e^a - 1)} - 1}{2(\alpha + 1)(e^a - 1)}, \tag{30}$$

which becomes independent of the binding free energies. We again note that these results are valid for $0 < \alpha < 1$ and the results for $\alpha > 1$ can be obtained by replacing α with $1/\alpha$. Moreover, in the case of unequal activation free energies, a represents the activation free energy of the more abundant species. $f^{\max}$ can be simplified further in two limiting cases of $a \to 0$ and $a \to \infty$ to

$$f^{\max} = \begin{cases} \dfrac{\alpha(3-\alpha)}{\alpha + 1}, & a \to 0, \\ \dfrac{2\alpha}{\alpha + 1}, & a \to \infty. \end{cases} \tag{31}$$

In the extreme case of $a \to \infty$ and $b_{AB} \to \infty$ such that $a - b_{AB}$ is finite, the polymerization transition corresponds to a sharp transition from a monomeric regime to a copolymer dominated regime. In this case, equal volume fractions of A and B monomers $[\alpha/(1 + \alpha)\Phi]$ are self-assembled and the excess of B monomers remains in the solution. The $f^{\max}$ values extracted from the numerical solution of the mass balance equations are presented in Fig. 3. They show excellent agreement with our theoretical predictions given by Eqs. (30) and (31) for all values of a and α.

Likewise, we also estimate the maximum mean degree of polymerization $\overline{N}^{\max}$ in the saturation regime for $J \to -\infty$,

$$\overline{N}^{\max} = \frac{1 + \alpha}{1 - \alpha}, \tag{32}$$

which only depends on the stoichiometric ratio and is valid for $0 < \alpha < 1$. The results for $\alpha > 1$ can be obtained by the transformation $\alpha \to 1/\alpha$. For $\alpha \neq 1$, at large overall volume fractions, nearly all the monomers of the minority species are polymerized into

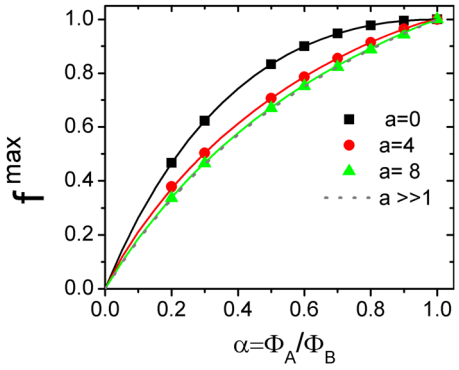

FIG. 3. The maximum fraction of polymerized material in the saturation limit, f^{max}, as a function of the stoichiometric ratio $\alpha = \Phi_A/\Phi_B < 1$ for different values of the activation free energies $a_A = a_B = a$, in the limit of $J \to -\infty$, where no binding between identical species occurs, i.e., $b_{AA} = b_{BB} \to -\infty$. The symbols show f^{max} values obtained from the numerical solution of the mass balance equations Eqs. (27) and (28) for the interspecies binding free energy $b_{AB} = b_{BA} = 14$ at high concentrations. The lines show our theoretical predictions given by Eqs. (30) and (31) confirming that f^{max} is independent of b_{AB}.

alternating copolymers that are capped at the ends by the majority species. As a result, the mean degree of polymerization saturates. Even under such conditions, due to entropic effects, the monomers of the minority species are never completely polymerized, meaning that there is always a monomeric pool. Notably, $\overline{N}^{max}$ becomes rather small when α significantly differs from unity.

We notice that Eq. (32) is identical to Carothers' equation[48] for the maximum degree of polymerization as a function of the comonomer ratio in the context of step-growth polymerization in the full conversion limit. However, our theoretical insights go beyond the description of a simple isodesmic or step-growth-like model and include cooperative supramolecular copolymerizations with high activation energies.[12] The latter are essential in rationalizing the experimental observations for the copolymerization of positively and negatively charged comonomers (Sec. V). Although $\overline{N}^{max}$ is independent of the activation free energy and only dependent on the stoichiometric ratio, the pace at which $\overline{N}$ approaches $\overline{N}^{max}$ with increasing Φ strongly depends on a as can be observed from Fig. 4(a).

Figure 4(a) presents the mean degree of polymerization $\overline{N}$ vs the overall volume fraction of monomers Φ at different stoichiometric ratios α and for two different values of the activation free energy. In perfect agreement with our theoretical estimate for $\alpha < 1$, $\overline{N}$ at high concentrations saturates to a value that is given by Eq. (32). Only for the $\alpha = 1$ case, the mean degree of polymerization grows indefinitely with Φ and it is described by the well-known square-root law[47] at large concentrations.

The mean degree of polymerization $\overline{N}$ defined by Eq. (18) is frequently used in theoretical calculations,[14,47] and it is of relevance to light scattering measurements. However, monomers are not considered in the average length of assemblies determined from transmission electron microscopy measurements. Therefore, it is useful to calculate a mean polymerization degree where only assemblies with $N \geq 2$ are included in the averaging. We denote such an average by $\overline{N}_p$, defined as

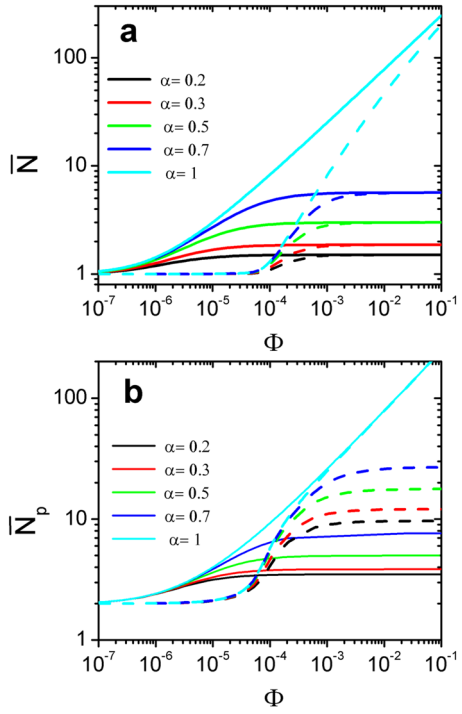

FIG. 4. The mean degree of polymerization defined by (a) Eq. (18) and (b) Eq. (33) as a function of overall concentration of monomers, Φ, at different stoichiometric ratios $\alpha = \Phi_A/\Phi_B < 1$, as given in the legends. The assumed values of the binding free energies are $b_{AA} = b_{BB} \to -\infty$ and $b_{AB} = b_{BA} = 14$ yielding $J \to -\infty$. The solid and dashed lines exhibit the results for activation free energies $a_A = a_B = a = 0$ and 4, respectively.

$$\overline{N}_p \equiv \frac{\sum_{N=2}^{\infty} N\rho(N)}{\sum_{N=2}^{\infty} \rho(N)}. \tag{33}$$

We have plotted $\overline{N}_p$ as a function of Φ in Fig. 4(b). Similar to $\overline{N}$, it saturates to a maximum value $\overline{N}_p^{max}$ for $\alpha < 1$, but its value now depends on the activation free energy. It is larger for cooperative copolymerization $a > 0$. The dependence of $\overline{N}_p$ on the stoichiometric ratio shows a good agreement with the experimentally reported trend for the average length of assemblies.[27] We can also find an analytical expression for it given as

$$\overline{N}_p^{max} = \frac{2 - \alpha + \sqrt{1 - 4(\alpha - 1)\alpha(e^a - 1)}}{1 - \alpha}, \tag{34}$$

which is in perfect agreement with the numerical results. These results demonstrate that at a fixed overall volume fraction of monomers, we can control the average length of polymers by tuning the stoichiometric ratio of the two components.

C. Critical concentration

The critical concentration describes the transition from conditions of minimal assembly to those characterized by a strong polymerization.[47,49] Different definitions for the critical concentration

Φ^* have been proposed in the literature.[14,47] In the simplest one, Φ^* is defined as the concentration at which half of the material is polymerized. In a more rigorous approach, Φ^* is defined as the concentration at which the volume fraction of free monomers as a function of the overall concentration saturates.[28,49] The critical concentration of a monodisperse system defined by the latter reads $\Phi_i^* = \exp(-b_{ii} + a_i)$.[14] In the strong-polymerization regime, i.e., at high volume fractions $\Phi \gg \Phi^*$, the fraction of polymerized material f obeys the simple relation $f = 1 - \Phi^*/\Phi$.[14] For small values of a_i, $f \approx 0.5$ at Φ^*, thus agreeing with the former definition. Moreover, in the limit $a_i \to \infty$ and $b_i \to \infty$ such that $-b_{ii} + a_i$ remains finite, Φ_i^* demarcates a true first order phase transition from a monomeric regime $f = 0$ to a fully polymerized regime $f = 1$. Here, we use the latter definition to determine the critical concentration of the two-component system in the strongly negative coupling limit. We obtain an analytical expression for the critical concentration Φ^* in the limit of $J \ll -1$ for the case that b_{ii} are positive and finite and the interspecies binding free energy is very large, i.e., $b_{AB} \gg b_{ii}$. *Similar to what is the case in the one-component system, at concentrations in excess of Φ^*, the volume fraction of free monomers saturates, in other words* $\Lambda_+ \to 1$.[28,47] Φ^* depends on the effective binding and activation free energies and the stoichiometric ratio.[28,47]

The conditions of polymerization transition for a bidisperse system are given by the following set of equations:[28]

$$\begin{aligned} &\Lambda_+(\mu_A^*, \mu_B^*) \to 1, \\ &\left.\frac{\partial \Lambda_+}{\partial H}\right|_{\substack{\mu_A=\mu_A^* \\ \mu_B=\mu_B^*}} = \frac{\alpha - 1}{\alpha + 1}, \end{aligned} \tag{35}$$

where μ_A^* and μ_B^* are the values of the chemical potentials at the critical concentration. Hence, Φ^* is given by the total volume fraction of free monomers,

$$\Phi^*(\alpha) = \mathbf{e}^{\mu_A^* + a_A} + \mathbf{e}^{\mu_B^* + a_B}. \tag{36}$$

Note that this definition of the critical concentration is only valid when $\Lambda_+ \to 1$ in the saturation limit of copolymerization. Therefore, it does not apply to the case of $b_{ii} \to -\infty$ and $\alpha \neq 1$ where Λ_+ at large concentrations saturates to $\Lambda_+^{\max} < 1$.

Taking into account the first two leading order terms of eigenvalues given in Eq. (22), we can find an analytical solution for Eq. (35) in the strongly negative coupling limit which results in

$$\Phi^*(\alpha) = \frac{(\Phi_A^* - \Phi_B^*)\left(\frac{\alpha-1}{\alpha+1}\right) + (\Phi_A^* + \Phi_B^*)\sqrt{\mathbf{e}^{4J} + \left(\frac{\alpha-1}{\alpha+1}\right)^2}}{1 + \sqrt{\mathbf{e}^{4J} + \left(\frac{\alpha-1}{\alpha+1}\right)^2}}. \tag{37}$$

For equal volume fractions of the two species, $\alpha = 1$, Eq. (37) gives $\Phi^*(1) = (\Phi_A^* + \Phi_B^*)(1 + e^{-2J})^{-1}$. Especially, for the case of equal activation free energies, $a_A = a_B = a$, it can be simplified to $\Phi^*(1) \approx 2\mathbf{e}^{-b_{AB}+a}$, which is identical to Φ_{AB}^* defined earlier for strictly alternating copolymers. For small and large values of α, the critical concentration simplifies to

$$\Phi^* = \begin{cases} \Phi_B^*(1 - \alpha), & \alpha \ll 1, \\ \Phi_A^*(1 - \alpha^{-1}), & \alpha \gg 1, \end{cases} \tag{38}$$

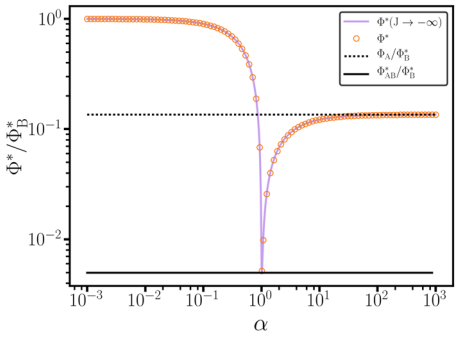

FIG. 5. The critical concentration, Φ^*, normalized by the critical concentration of species B, Φ_B^*, as a function of the stoichiometric ratio $\alpha = \Phi_A/\Phi_B$. The numerical solution of Eq. (35) is displayed by orange open circles, and the analytical result of Eq. (37) is shown by a purple solid line. The binding and activation free energies used are $b_{AA} = 10$, $b_{BB} = 8$, $b_{AB} = b_{BA} = 14$, and $a_A = a_B = 1.5$, yielding $\Phi_A^* = 2.03 \times 10^{-4}$, $\Phi_B^* = 1.50 \times 10^{-3}$, and $\Phi_{AB}^* = 7.45 \times 10^{-6}$.

where Φ_A^* and Φ_B^* are the critical concentrations of homopolymers composed of A and B species, respectively. These equations show that Φ^* approaches the critical concentration of the homopolymer of the more abundant species in the appropriate limit.

To investigate the validity of Eq. (37), we numerically solve the set of Eq. (35) for a sufficiently negative coupling constant $J = -5/2$ to obtain $\Phi^*(\alpha)$ as plotted in Fig. 5. For all the stoichiometric values α, we find excellent agreement between the numerical and analytical solutions. Additionally, we find that the strong coupling limit critical concentration, described by Eq. (37), provides a good description of numerical results for all coupling constants $J < -1$.

IV. COPOLYMERIZATION BEHAVIOR PREDOMINATED BY ALTERNATING CONFIGURATIONS

Having discussed the copolymerization with strictly alternating order, i.e., the antiferromagnetic regime in the $J \to -\infty$ limit, we now discuss the numerical solution of the mass-balance equations for a finite and negative coupling constant. Numerical solutions were obtained from a Python script where the SciPy function *scipy.optimize.fsolve*[50–52] was made use of (see the supplementary material). We investigate the polymerization behavior and composition of copolymers as a function of the overall volume fraction and stoichiometric ratio. Especially, we introduce an order parameter which quantifies the overall fraction of polymers with perfect alternating order.

A. Fraction of polymerized material and mean degree of polymerization

We fix the values of the free energies such that $b_{AB} > b_{AA} > b_{BB}$, and we focus on the polymerization behavior for stoichiometric ratios $0 < \alpha \leq 1$. We note that the labels of the species, A and B, are *a priori* arbitrary and the above conditions determine the specific labels of the two species. Therefore, the results for $\alpha > 1$ can be simply obtained through an interchange of species labels and our presented analysis is without loss of generality. We set the binding free energy

values to $b_{AA} = 10$, $b_{BB} = 8$, and $b_{AB} = b_{BA} = 14$. These values give rise to $J = -5/2$, which is sufficiently negative to expect the alternating order to be the predominant morphology. Moreover, we choose equal activation free energy values for the two species $a_A = a_B = 1.5$ to reduce the number of parameters. They are chosen small enough to allow us to obtain accurate numerical results. As discussed in Sec. III B, the activation free energy value affects the sharpness of the transition from the monomeric to the polymeric dominated regime but does not alter the overall self-assembly behavior.

We determine the chemical potentials μ_i by solving the mass-balance equations Eqs. (16) and (17) numerically from which we calculate the volume fraction of free monomers in the solution as $\phi_i^m = \exp(\mu_i + a_i)$. In Fig. 6, we have depicted ϕ_i^m as a function of the overall volume fraction Φ at different stoichiometric ratios $0 < \alpha \leq 1$. We find that at very low concentrations, $\Phi < 10^{-5}$, the ratio of free monomer volume fractions $\alpha^f \equiv \phi_A^m/\phi_B^m$ is almost identical to α. However, at larger concentrations and for $\alpha < 1$, the value of ϕ_A^m drops considerably such that $\alpha^f \ll \alpha$. Even for the case of $\alpha = 1$, we notice that $\Phi_A^m < \Phi_B^m$ when $\Phi > 10^{-4}$ because of a greater tendency of species A to homopolymerize. We have also indicated the values of ϕ_i^m at the associated critical concentrations for each α. Consistent with the definition of the critical concentration in Sec. III C, at the critical concentration, the total volume fraction of free monomers $\phi_A^m + \phi_B^m$ approaches its saturation limit.

We next examine the fraction of polymerized material f as a function of the overall volume fraction Φ presented in Fig. 7(a) for various stoichiometric ratios $0 < \alpha \leq 1$. Here, f_A and f_B represent the fraction of polymerized material for homopolymers consisting of A and B species, respectively. They correspond to the results for the limiting cases of $\alpha = \infty$ and $\alpha = 0$ that are determined from the mass balance equation given in Eq. (21). For comparison, we have also presented the fraction of polymerized material in the strongly negative coupling limit, i.e., $b_{BB} = b_{AA} \to -\infty$, and with otherwise identical free energy parameters. These curves, depicted by open symbols, are obtained by solving the mass-balance equations [Eqs. (27) and (28)]. f_{AB}, shown by the dashed line, depicts the results for the special case of quasihomopolymers made of (AB) monomers at $\alpha = 1$, and it is obtained from solving Eq. (29). Figure 7(a) shows that the fraction of polymerized material is bound by the polymerization curves f_{AB} and $f_B(f_A)$ for $\alpha < 1$ ($\alpha > 1$). The polymerization behavior of copolymers with a finite negative coupling constant at high concentrations is notably different from that of strictly alternating copolymers. In the latter case, f saturates to a value $f^{\max}(\alpha) < 1$, unless $\alpha = 1$. However, at lower concentrations, the polymerization curves are identical to those of strictly alternating copolymers. This agreement suggests that copolymers at low volume fractions have a predominantly alternating order.

Our conclusions are further supported by the concentration dependence of the mean degree of polymerization presented in Fig. 7(b). We note that at low and intermediate concentrations, $\overline{N}$ of copolymers with a finite coupling constant (filled symbols) agrees

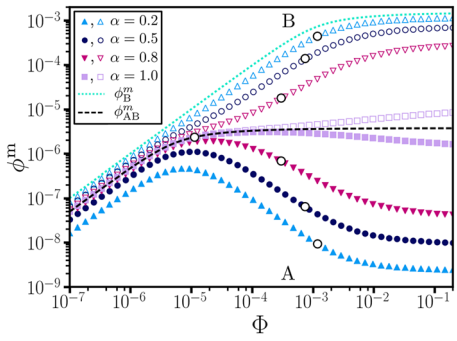

FIG. 6. The volume fraction of free monomers ϕ^m for species A (closed symbols) and species B (open symbols) as a function of the overall volume fraction $\Phi = \Phi_A + \Phi_B$ at different stoichiometric ratios $\alpha = \Phi_A/\Phi_B$, as given in the legend. The volume fractions of the free monomers at the critical concentrations are depicted by closed white circles. The dotted line shows the free monomer volume fraction for B-homopolymers ϕ_B^m in the case of one-component system, and the dashed line shows the special cases of strictly alternating AB-copolymers ϕ_{AB}^m. The values of the activation energies are $a_A = a_B = 1.5$ and of the binding free energies are $b_{AA} = 10$, $b_{BB} = 8$, and $b_{AB} = b_{BA} = 14$, resulting in a negative coupling constant $J = -5/2$. Note that the $\alpha = 1$ case loses A-B symmetry since $b_{AA} > b_{BB}$.

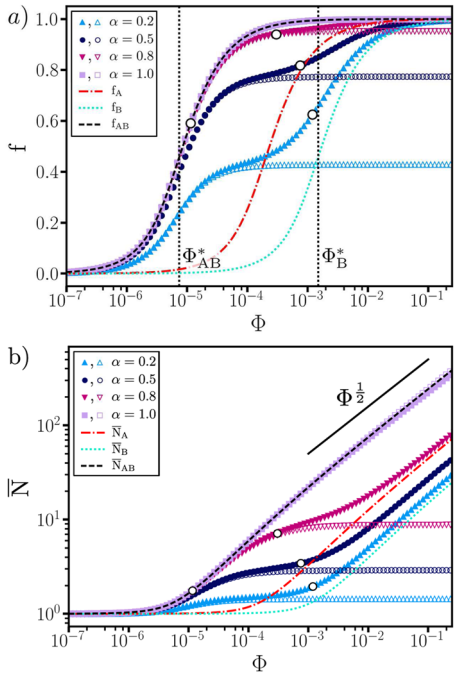

FIG. 7. (a) Fraction of polymerized material f and (b) mean degree of polymerization $\overline{N}$ as a function of the overall volume fraction of dissolved monomers $\Phi = \Phi_A + \Phi_B$ at different stoichiometric ratios as given in the legends. The values of f and $\overline{N}$ at the corresponding critical concentrations are depicted by closed white circles. The filled symbols correspond to polymerization curves of two component self-assemblies with activation free energies $a_A = a_B = 1.5$ and binding free energies $b_{AA} = 10$, $b_{BB} = 8$, and $b_{AB} = b_{BA} = 14$, yielding a coupling constant $J = -5/2$. The results for homopolymers consisting of A species (f_A and $\overline{N}_A$, dotted-dashed lines) and of B species (f_B and $\overline{N}_B$, dotted lines) and the strictly alternating copolymer consisting of repeat units of (AB) (f_{AB} and $\overline{N}_{AB}$, dashed lines) are also presented. Furthermore, the open symbols show f and $\overline{N}$ in the strongly negative coupling limit, $J \to -\infty$ when $b_{ii} \to -\infty$, computed from the numerical solutions of Eqs. (27) and (28), with otherwise identical parameters.

with those in the strongly negative coupling limit (open symbols). This figure further confirms that at the early stages of polymerization, short alternating polymers are formed. At very low volume fractions $\Phi \lesssim \Phi^*_{AB}$, the solution is mainly in a monomer-dominated state and $\overline{N} \approx 1$. At the intermediate volume fractions, $\overline{N}$ monotonically increases with a slope that depends on α and Φ. At high Φ, the polymer assemblies follow the well-known square root law found for homopolymers[47] but with a coefficient that increases with α. We have also marked the values of the fraction of polymerized material and the average degree of polymerization at $\Phi^*(\alpha)$ in Figs. 7(a) and 7(b), respectively. As can be seen, the critical concentration for the one-component system of B-homopolymers and the two-component system with $\alpha = 1$ coincides with the volume fraction at which about 50% of the material is polymerized. However, for stoichiometric ratios different from unity, the critical concentration does not demarcate the concentration at which the fraction of self-assembled material departs significantly from zero. Rather, it determines the polymerization regime where homopolymerization takes over the copolymerization with predominantly alternating order. This finds its cause in our definition of the critical concentration that determines the volume fraction for which the total density of free monomers saturates.

B. Spatial correlation function

To characterize the extent of alternating (antiferromagnetic) order within assemblies of size N, we calculate the spatial spin correlation function. The spatial correlation function $\langle S_i S_j \rangle$ describes the correlation between spins at lattice sites i and j or, equivalently, the correlation between the average occupancy of the two species at lattice sites i and j. It is also related to the probability $P_{ij} = 1/2(1 + \langle S_i S_j \rangle)$ that the spins at sites i and j have the same value,[46] or equivalently, the sites i and j are occupied by the same species. For a copolymer with perfect alternating order, $\langle S_i S_j \rangle = (-1)^{|j-i|}$. The spatial correlation function of an Ising model with open boundary conditions, in the general case, can be obtained using the standard transfer matrix method;[46] see the Appendix for details. Assuming $i \le j \le N$, it is given by

$$\langle S_i S_j \rangle = \frac{1}{1 + e^{4J}\sinh^2(H)} \Bigg(e^{4J}\sinh^2(H) + \frac{x_+\lambda_+^{N-1-j+i}\lambda_-^{j-i} + x_-\lambda_-^{N-1-j+i}\lambda_+^{j-i}}{x_+\lambda_+^{N-1} + x_-\lambda_-^{N-1}} + \frac{\lambda_+^{i-1}\lambda_-^{N-i} - \lambda_-^{i-1}\lambda_+^{N-i} + \lambda_-^{j-1}\lambda_+^{N-j} - \lambda_+^{j-1}\lambda_-^{N-j}}{x_+\lambda_+^{N-1} + x_-\lambda_-^{N-1}} \times e^{2J}\sinh(H)\sqrt{x_+x_-} \Bigg), \tag{39}$$

which is positive for spins with the same sign (identical species) and negative for spins of the opposite sign (distinct species). We note that in addition to a term depending on the external field H, the correlation function includes terms which depend on the distance between the two sites $|j - i|$ and terms which depend on the specific position of sites i and j.

In the strongly negative coupling limit such that $e^{2J}\sinh(H) \ll 1$, the correlation function simplifies to

$$\langle S_i S_j \rangle = \frac{x_+\lambda_+^{N-1-j+i}\lambda_-^{j-i} + x_-\lambda_-^{N-1-j+i}\lambda_+^{j-i}}{x_+\lambda_+^{N-1} + x_-\lambda_-^{N-1}}. \tag{40}$$

Noting that $(\lambda_-/\lambda_+)^N \ll 1$ for $N \gg 1$, the correlation function in the thermodynamic limit becomes independent of boundary conditions and can be further simplified to

$$\langle S_i S_j \rangle = \left(\frac{\lambda_-}{\lambda_+}\right)^{j-i}. \tag{41}$$

Particularly, in the limit $J \to -\infty$, using Eq. (22) for the eigenvalues, it becomes an oscillatory function as $\langle S_i S_j \rangle = (-1)^{j-i}$, indicating that the assemblies have perfect alternating order. Re-expressing $\langle S_i S_j \rangle$ as $\exp\left[-(j-i)\ln\left(\frac{\lambda_+}{\lambda_-}\right)\right]$, we notice that the long chain correlation function decays exponentially, $\langle S_i S_j \rangle = \exp[-(j-i)/\xi_0]$, with a correlation length ξ_0 given by

$$\xi_0^{-1} = \ln\left(\frac{\lambda_+}{\lambda_-}\right). \tag{42}$$

Using the form of eigenvalues in the strong coupling limit $-J \gg 1$, given by Eq. (22), leads to

$$\xi_0^{-1} = \ln\left(\frac{\cosh(H)e^{2J} + 1}{\cosh(H)e^{2J} - 1}\right) \approx 2\cosh(H)e^{2J} + i\pi, \tag{43}$$

where in the last expression, the identity $\ln(-1) = i\pi$ is used and we have assumed $\cosh(H)\, e^{2J} \ll 1$. This expression further simplifies to $\xi_0^{-1} = \ln[\coth(J)]$ for $H = 0$, and it diverges for $J \to -\infty$. Consequently, the correlation function in the large N and $-J$ limits can be written as

$$\langle S_i S_j \rangle = \exp[-2(j-i)\cosh[H)e^{2J}]\cos[(j-i)\pi]. \tag{44}$$

It is an exponentially decaying function modulated by a cosine wave with a periodicity of 2, reflecting the alternating order of the Ising antiferromagnet.

Having discussed the behavior of the correlation function in the strong coupling limit, next we discuss its behavior for copolymers obtained for different stoichiometric ratios at a low and a high volume fraction. Under general conditions, the correlation function depends on the distance between the two sites $|j - i|$ and on the specific positions of the two sites i and j. Setting $i = 1$, we have plotted the correlation function as a function of the normalized distance $|j - i|/\overline{N}_p$ in Fig. 8 for 4 stoichiometric values $\alpha = \{0.2, 0.5, 0.8, 1.0\}$, where $\overline{N}_p$ is defined by Eq. (33). Figure 8(a) presents the correlation function at the low volume fraction $\Phi = 10^{-4}$, and Fig. 8(b), at the high volume fraction $\Phi = 10^{-2}$. Additionally, we have included the exponentially decaying function $\exp(-\xi_0^{-1}|j - i|/\overline{N}_p)$ from Eq. (44). At the low volume fraction, the average polymer lengths corresponding to the given stoichiometric values are $\overline{N}_p = \{5, 7, 8.5, 9.3\}$, respectively. For these short polymers of length $\overline{N}_p$, Fig. 8(a) demonstrates that the spins remain correlated. Hence, the copolymers are in predominantly strictly alternating configurations. Figure 8(b) shows the correlation function at the high volume fraction, where the average polymer lengths are $\overline{N}_p = \{13, 19, 33, 117\}$ for $\alpha = \{0.2, 0.5, 0.8, 1.0\}$, respectively. We observe that the correlations decay toward the middle of the assemblies and increase near the end. This nonmonotonic behavior results from the finite size of assemblies and a large

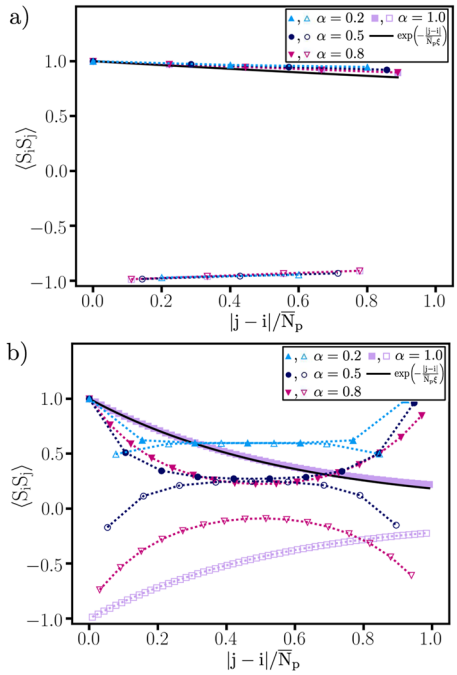

FIG. 8. The correlation function between spins at sites $i = 1$ and $j \geq 1$, $\langle S_i S_j \rangle$, plotted vs the separation distance $|j - i|$ normalized by the assembly length $\overline{N}_p$ for stoichiometric ratios $\alpha = \{0.2, 0.5, 0.8, 1.0\}$ at (a) $\Phi = 10^{-4}$ and (b) $\Phi = 0.024$. Here, $\overline{N}_p$ is the average length of assemblies at each concentration and stoichiometric ratio. The corresponding values are $\overline{N}_p = \{5, 7, 9, 9\}$ at $\Phi = 10^{-4}$ and $\overline{N}_p = \{13, 19, 33, 117\}$ at $\Phi = 0.024$ for $\alpha = \{0.2, 0.5, 0.8, 1.0\}$, respectively. $\langle S_i S_j \rangle$ for $j - i$ even and odd are shown with closed and open symbols connected by dotted lines, respectively. The correlation function for $\alpha = 1$ and even distances approaches to that of the thermodynamic limit $N \to \infty$ at large J and $H \approx 1$ given by Eq. (41) which is shown by solid lines.

disparity in the population of the two species, which leads to a large $\Delta\mu$ (see Fig. 6) and thus a nonzero magnetic field. Especially, for $\alpha = 0.2$, with $\overline{N}_p = 13$, the spins remain correlated and the ferromagnetic ordering seems to be prevalent for such short assemblies. These results demonstrate that at higher volume fractions, for $\alpha < 1$, the copolymers of size $\overline{N}_p$ are unlikely to be in strictly alternating configurations, as in fact will be demonstrated in Subsection IV C.

C. Composition of supramolecular copolymers

To provide a quantitative insight into the composition of copolymers, we determine the fraction of perfectly alternating copolymers and B-homopolymers as a function of concentration and assembly length. For a given supramolecular polymer length N, the fraction of strictly alternating copolymers is determined by

$$f_{\text{alt}}(N) = \frac{\sum_{\text{config}} \exp[-\mathcal{H}_{alt}(N)]}{Z_N}, \tag{45}$$

where Z_N is the copolymer partition function given by Eq. (7) and $\mathcal{H}_{alt}(N)$ is the free energy of an alternating configuration of size N. Summing over all alternating configurations in the numerator yields $Z^{\text{even}}_{N>1}$ and $Z^{\text{odd}}_{N>1}$, defined by Eqs. (25) and (26), for even and odd degrees of polymerization, respectively. From now on, we refer to both as Z^{alt}_N. Likewise, the fraction of B-homopolymers is obtained as

$$f_{\text{B-homo}}(N) = \frac{\exp[-\mathcal{H}_{\text{B-homo}}]}{Z_N} = \frac{\exp[\mu_B N + (N-1) b_{BB}]}{Z_N}, \tag{46}$$

where $\mathcal{H}_{\text{B-homo}}$ is the free energy of a homopolymer of size N.

Figures 9(a) and 9(b) present the fraction of strictly alternating copolymers $f_{\text{alt}}(N)$ as a function of the assembly length N at two concentrations $\Phi = 10^{-4}$ and $\Phi = 10^{-2}$ and for different stoichiometric ratios. Two important conclusions can be drawn from these results. First, the fraction of alternating polymers with an even degree of polymerization is smaller than the fraction of those with an odd degree of polymerization, except for the case of $\alpha = 1$ and $\Phi = 10^{-4}$. Notably, the difference between populations of odd and even numbered alternating copolymers is larger for smaller α and it reflects the lack of the scarcer A species. The more abundant B species can have a greater contribution to polymerization by forming alternating copolymers of the form $B(AB)_{2N}$. Second, the fraction of perfectly alternating copolymers decreases with N and this decrease is stronger for smaller stoichiometric ratios. Interestingly, $f_{\text{alt}}(N)$ for stoichiometric ratios $\alpha = 0.2$ and 0.5 exhibits a two-step decay: an initial rapid decay for short copolymers and a second slower exponential decrease for longer assemblies. At the higher concentration, where the fraction of polymerized material is larger, the fraction of alternating copolymers shows a stronger decrease with N, even for the case of equal concentrations, $\alpha = 1$.

The observed behavior is consistent with the picture arising from the Ising correlation length discussed earlier at $H \approx 0$, where we have $\xi_0 \approx \exp(-2J)/2 \approx 74$. At low and intermediate concentrations where $\overline{N}_p < \xi_0$, the short assemblies have a nearly perfect alternating order. However, upon an increase in the concentration and growth of mean degree of polymerization, for long assemblies with $N \gg \xi_0$, the combinatorial factor can benefit from the formation of alternating copolymers with defects. Additionally, at sufficiently high Φ for $\alpha < 1$, the excess of B species can form homopolymers. The fraction of B-homopolymers vs N is shown in Figs. 9(c) and 9(d) for $\Phi = 10^{-4}$ and $\Phi = 10^{-2}$, respectively. As can be seen at the lower concentration, there exist almost no homopolymers, whereas at the higher concentration for $\alpha < 1$, a notable fraction of homopolymers appears. Evidently, at the smaller α with a larger excess of B species, longer homopolymers are more probable.

Next, we calculate the total fraction of perfectly alternating copolymers and homopolymers as a function of the overall concentration of monomers. The total fraction of perfectly alternating copolymers can be obtained as

$$f^{\text{tot}}_{\text{alt}} \equiv \frac{\sum_{N=2}^{\infty} \rho(N) f_{\text{alt}}(N)}{\sum_{N=2}^{\infty} \rho(N)} = \frac{\sum_{N=2}^{\infty} Z^{alt}_N}{\sum_{N=2}^{\infty} Z_N}. \tag{47}$$

Using formulas for convergent geometric series, both sums can be evaluated to express $f^{\text{tot}}_{\text{alt}}$ in terms of the chemical potentials μ_i. Similarly, the total fraction of B-homopolymers is given by

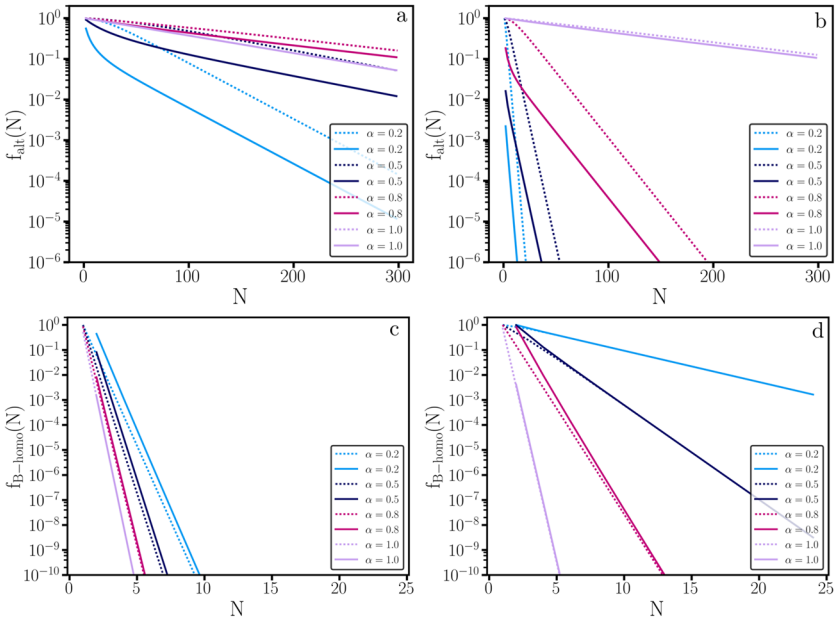

FIG. 9. [(a) and (b)] The fraction of copolymers of length N with perfect alternating order relative to all polymers with the same length, f_{alt}, as defined by Eq. (45), and [(c) and (d)] the fraction of N-mer B-homopolymers relative to all copolymers with the same length $f_{B\text{-homo}}(N)$, as defined by Eq. (48), plotted against N at different stoichiometric ratios α given in the legends. The dotted and solid lines correspond to polymers with odd and even degrees of polymerization, respectively. The overall monomer concentration is $\Phi = 10^{-4}$ in panels (a) and (c) and is $\Phi = 10^{-2}$ in panels (b) and (d). The values of the activation and the binding free energies are $a_A = a_B = 1.5$ and $b_{AA} = 10$, $b_{BB} = 8$, and $b_{AB} = b_{BA} = 14$, resulting in $J = -5/2$.

$$f^{\text{tot}}_{\text{B-homo}} \equiv \frac{\sum_{N=2}^{\infty} \rho(N) f_{\text{B-homo}}(N)}{\sum_{N=2}^{\infty} \rho(N)} = \frac{\sum_{N=2}^{\infty} \exp[\mu_B N + (N-1) b_{BB}]}{\sum_{N=2}^{\infty} Z_N}, \tag{48}$$

which can be straightforwardly evaluated.

Figure 10 shows $f^{\text{tot}}_{\text{alt}}$ and $f^{\text{tot}}_{\text{B-homo}}$ as a function of the overall volume fraction at different stoichiometric ratios. At low volume fractions $\Phi \lesssim \Phi^*_{AB}$, where most of the material is in the monomeric form and only few short polymers are formed, $f^{\text{tot}}_{\text{alt}} \approx 1$ and $f^{\text{tot}}_{\text{B-homo}} \approx 0$. Hence, we conclude that at low Φ, the majority of assemblies are in an alternating configuration. For $\Phi > \Phi^*_{AB}$, the fraction of perfectly alternating copolymers monotonically decreases with the concentration, whereas the fraction of B-homopolymers vs concentration exhibits a maximum for $\alpha < 1$. The maximum in $f^{\text{tot}}_{\text{B-homo}}(\Phi)$ appears at volume fractions where the concentration of excess B-monomers becomes comparable to Φ^*_B. At high Φ, $f^{\text{tot}}_{\text{alt}} + f^{\text{tot}}_{\text{B-homo}} < 1$ which shows that the system contains alternating copolymer and homopolymer configurations with defects in addition to strictly alternating copolymers and pure homopolymers. The existence of such configurations reflects that the mixing entropy overcomes the energetically unfavorable compositions, particularly for long assemblies where the combinatorial factor is larger.

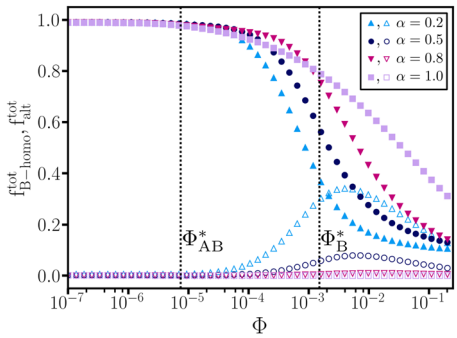

FIG. 10. The total fraction of copolymers with perfect alternating order $f^{\text{tot}}_{\text{alt}}$ (closed symbols) and the total fraction of homopolymers consisting of B species $f^{\text{tot}}_{\text{B-homo}}$ (open symbols) as a function of the overall volume fraction of dissolved monomers $\Phi = \Phi_A + \Phi_B$ at different stoichiometric ratios $\alpha = \Phi_A/\Phi_B$ as given in the legend. The values of the activation and binding free energies are $a_A = a_B = 1.5$ and $b_{AA} = 10$, $b_{BB} = 8$, and $b_{AB} = b_{BA} = 14$, resulting in $J = -5/2$.

V. LINK TO EXPERIMENTAL OBSERVATIONS

In this section, we rationalize the experimental observations on the copolymerization of positively and negatively charged comonomers[25,26] on the basis of our theoretical insights. As briefly discussed in Sec. I, the comonomer species with complementary charges contain three identical amphiphilic oligopeptide arms that possess C_3 symmetry. Each arm has 2 charged groups, and therefore, a monomer has at most a total charge of 6 e, depending on the pH conditions. The oligopeptide design of each arm is based on a phenyl alanine and methionine sequence for the hydrophobic amino acid, alternated with a cationic lysine (blue comonomer A in Fig. 1) or anionic glutamic acid moiety (green comonomer B in Fig. 1). The terminal hydrophilic dendritic triethylene glycol chains are introduced to guarantee a high colloidal stability of the copolymers in a neutral buffer of physiological ionic strength. Further details on the synthesis of the C_3 symmetrical comonomers can be found in Ref. 53.

At neutral pH values, the two species are oppositely charged and they copolymerize into linear aggregates.[54] The electrostatic

interactions between the monomers enhance the binding between the A and B species with complementary charges and reduce the binding free energy between identical species. Therefore, the copolymerization of this system corresponds to the regime where interspecies binding is favored over homopolymerization, leading to a strongly negative coupling constant J in the language of our theory. To make the link between the theory and the experiments more quantitative, we provide a rough estimate of the effective coupling constant.

Due to the similar chemical architecture of the two species, we assume that the bare binding free energies in the uncharged state are equal, i.e., $b_{ij} = b_0$. In the charged state, the binding free energy values are modified due to electrostatic interactions. The magnitude of electrostatic free energy between any two neighboring monomers is given by $b_{\rm el}$ because the two species have equal charge magnitudes. As a result, the effective binding free energies modify to $b_{AA} = b_{BB} = (b_0 - b_{\rm el})$ and $b_{AB} = b_{BA} = (b_0 + b_{\rm el})$, leading to a coupling constant $J = -b_{\rm el}$; see Eq. (4). We estimate the electrostatic contribution based on the Debye-Hückel theory[55] for pair interactions between pointlike charges in an electrolyte as $b_{\rm el} = \lambda_B q^2 \exp(-\ell/\lambda_D)/\ell$, where q represents an effective charge valency and ℓ is the distance between the monomers. $\lambda_B \equiv e^2/(4\pi\epsilon k_B T)$ is the Bjerrum length in which e is the elementary charge and ϵ is the solvent permittivity. λ_D represents the Debye screening length, which depends on the ionic strength of the buffer solution.[55]

For the system discussed above, we expect $q < 6\ e$ due to projection from the discotic surface charge density into a pointlike charge distribution along the linear assemblies and electrostatic screening resulting from counterion condensation.[56] We estimate it to be in the range $3 < q < 6$ and the Debye screening length to be about $\lambda_D \approx 1$ nm under our experimental conditions. The Bjerrum length at room temperature is $\lambda_B \approx 0.7$ nm, and the spacing between monomers is $\ell = 0.47$ nm, on the basis of WAXS measurements.[57] Using these values, we estimate the electrostatic energy to be in the range $8.3 < b_{\rm el} < 33$ leading to a large negative $-33 < J < -8.3$. Hence, the correlation length 3.8×10^6 nm $< \xi_0 < 1.08 \times 10^{28}$ nm is so large that it favors strictly alternating copolymer configurations. Accordingly, homopolymerization will only take place if $b_0 > b_{\rm el}$; otherwise, the electrostatic repulsion will disfavor any binding between identical species. Experimentally, we do not observe any homopolymerization for either of the species around neutral pH values where both species are charged; see Fig. S4 of the supplementary material. Therefore, we conclude that our experimental system falls into the strongly negative coupling regime where copolymerization is favored over homopolymerization; see Sec. III. To test this hypothesis, we have measured the fraction of self-assembled material in the experimentally accessible range of concentrations. We particularly compare the maximum fraction of self-assembled material obtained from Eq. (30) with the experimental values.

In the experiments, the fraction of polymerized material f is obtained by circular dichroism (CD) spectroscopy where the normalized value for the molar circular dichroism $\Delta\epsilon$ is plotted as a function of the monomer stoichiometric ratio. We have previously shown that $\Delta\epsilon$ scales linearly with the fraction of polymerized material.[26,27,54] The feed titrations were performed in a 2 mm cuvette using separately prepared solutions of both monomers at pH 6.0 at a total monomer concentration of 6×10^{-5}M while monitoring the maximum of the negative CD band at a wavelength of 220 nm. The fraction of polymerized material was estimated by normalizing the intensity of the polymer specific CD band at 220 nm, where $f = 0$ refers to the monomeric state and $f = 1$ to the fully polymerized state. For the monomer species used in our experiments, the fraction of polymerized material for $\alpha = 1$ at neutral pH as well as homopolymers of species A at pH = 11.5 and species B at pH = 3 was measured for concentrations c in the range $2 < c < 100\ \mu$M. In all the cases, we find that f is constant in the measured concentration range, indicating that the corresponding critical concentrations are very low $\Phi^* < 10^{-5}$ and below the sensitivity limits of our circular dichroism setup; see Figs. S5–S10 of the supplementary material. Recalling that in the strong coupling regime $\Phi^*(1) \approx 2e^{-b_{AB}+a}$, these data confirm our inference that the interspecies binding is indeed very large. Moreover, we confirm the extraordinary high stability of the supramolecular copolymers by performing dilution and denaturation experiments with a chemical denaturant acetonitrile CH_3CN as the organic solvent. We were not able to observe disassembly into monomeric species by optical spectroscopy; see Figs. S11–S15 of the supplementary material. Thus, we conclude that the combination of hydrophobic shielding with Coulomb interactions and hydrogen bonding increases the stability of the copolymers A and B both in water, as well as in water-acetonitrile mixtures, compared to the homopolymers of A or B.

As obtaining the fraction of polymerized material below the saturation limit is experimentally challenging, we instead focus on the maximum fraction of self-assembled material extracted from the CD measurements. We measured the value of the CD signals as a function of the relative volume fraction of species A with respect to the overall volume fraction of monomers in the solution, $\Phi_A/\Phi \equiv \alpha/(\alpha + 1)$, at a fixed overall concentration 60 μM. The experimentally estimated fraction of polymerized material in the saturation regime is shown in Fig. 11. It clearly shows that the fraction of polymerized material varies strongly with the feed ratio x. As discussed in Sec. III B, in the strongly negative coupling limit, the

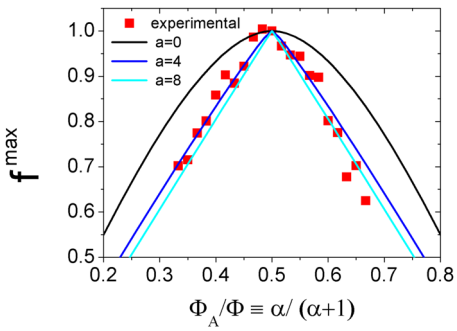

FIG. 11. Fraction of polymerized material in the saturation limit $f^{\rm max}$ plotted against the volume fraction of species A relative to the overall volume fraction of dissolved monomers, denoted by $\Phi_A/\Phi \equiv \alpha/(\alpha + 1)$. The experimental data are obtained from the CD measurements at a wavelength of 220 nm for a mixture of glutamic acid derivatives (negatively charged) and lysine derivatives (positively charged) as comonomers with a total concentration of 60 μM at pH 6.0. The solid lines show the theoretical prediction for $f^{\rm max}$ given by Eq. (30) at different activation free energies.

fraction of polymerized material reaches a maximum value $f^{\max}$ that depends on the stoichiometric ratio α and activation free energy a as given by Eq. (30). In Fig. 11, we have also included the theoretical prediction of $f^{\max}$. We find excellent agreement between the experimental and theoretical trends for large activation free energies $4 < a < 8$. These results confirm our hypothesis that the predominant configuration of assemblies is the alternating configuration and homopolymerization is entirely suppressed due to the repulsive electrostatic interactions between identical species. Another important conclusion that can be drawn is that the supramolecular copolymerization is highly cooperative and takes place via a nucleation-elongation mechanism.[27] We believe these interpretations to be valid even though our model only takes into account nearest neighbor interactions. The electrostatic interactions in the solution are rather short-ranged due to the screened nature of electrostatic interactions, $\lambda_D \approx 2\ell$. Moreover, the effect of electrostatic interactions with monomers beyond the adjacent neighbors could be captured by a renormalization of the interspecies binding free energy.[44]

The agreement between theory and experiments can be further tested by comparing the average length of self-assemblies extracted from transmission electron microscopy (TEM) with our theoretical predictions in the strong coupling regime. The number average length L_n of copolymers with stoichiometric ratios $\alpha = 0.5$, 1, and 2 was obtained for solutions at a total comonomer concentration of 5×10^{-5}M ($\Phi \approx 2 \times 10^{-4}$)[27] approaching the saturation regime. Assuming an intermonomer distance of 0.47 nm,[57] the mean length of copolymers was estimated as summarized in Table I. Our theory predicts that in the strong coupling limit, the mass balance equations only depend on 3 parameters a_A, a_B, and b_{AB} that can be adjusted to fit the values of $\overline{N}_p$ at the three different stoichiometric ratios. In particular, the maximum average length of copolymers $\overline{N}_p$ with $\alpha \neq 1$ in the saturation limit only depends on α and the activation free energy of the more abundant species, as given by Eq. (34). Fitting the experimental data with our model leads to an estimate of $a_A = 8.0$, $a_B = 8.5$, and $b_{AB} = 19.3$. We find good agreement between our theoretical and experimental results; see Table I. These values of the activation free energies are in agreement with our foregoing estimate based on the maximum fraction of polymerized material shown in Fig. 11. At stoichiometric ratios close to 1, we expect $\overline{N}_p$ to increase indefinitely with the overall concentration. Using our estimates of $\Phi \approx 2 \times 10^{-4}$, $a_A = 8.0$, $a_B = 8.5$, and choosing $b_{AB} = 19.3$, we obtain $\overline{N}_p = 142$ which is in agreement with the experimental result.

TABLE I. The average length of copolymer assemblies L_n and average degree of polymerization $\overline{N}_p$ at $\Phi \approx 2 \times 10^{-4}$ for three stoichiometric ratios α obtained from TEM measurements (experiment) and from our calculations in the strong coupling limit at $\Phi = 2 \times 10^{-4}$ using Eq. (33) with $a_A = 8.0$, $a_B = 8.5$, and $b_{AB} = 19.3$ (theory).

	Experiment		Theory	
α	L_n (nm)	$\overline{N}_p$	$\overline{N}_p$	$\overline{N}_p^{\max}$
1/2	50	106	104	143
1	66	140	142	...
2	42	89	90	112

VI. DISCUSSION AND CONCLUSIONS

We have examined the supramolecular self-assembly behavior of a two-component system under the conditions that interspecies binding is favored over binding between identical species. Our theoretical framework is based on the self-assembled nearest neighbor Ising model with a negative (antiferromagnetic) coupling constant. In the strongly negative coupling limit, i.e., $J \ll -1$, our model reduces to that of strictly alternating copolymers. The polymerization is maximal for equal volume fractions of the two species ($\alpha = 1$). For unequal volume fractions, the maximum fraction of polymerized material, $f^{\max}$, is smaller than unity because an excess of the more abundant species remains in the monomeric form. $f^{\max}$ and the maximum mean length of copolymers depend not only on the stoichiometric ratio α but also on the activation free energies. Hence, at a fixed overall monomer volume fraction, the mean degree of polymerization can be controlled by changing the stoichiometric ratio. We have also obtained the functional dependence of the critical concentration, Φ^*, on the stoichiometric ratio in this limit. The critical concentration of copolymers with sufficiently negative J scales as $\Phi^* \sim \exp(2J)$ at stoichiometric ratios close to one, and it is strikingly smaller than the critical concentration of either of the homopolymers. The stoichiometric dependence of the critical concentration of predominantly alternating copolymers is notably different from the case of self-assembly predominated by blocky ordering $J \gg 1$. In the latter case, the critical concentration is bound by the critical concentration of the two species and monotonically changes from one to the other $\Phi_B^* < \Phi^* < \Phi_A^*$.[28]

Investigating the copolymerization behavior for a finite and sufficiently negative coupling constant, we find that the numerically obtained critical concentration shows good agreement with our analytical results in the strong coupling limit. Moreover, the copolymerization behavior up to moderate volume fractions is similar to that of strictly alternating copolymer configurations. However, at larger volume fractions well beyond Φ^*, the copolymers lose their strict alternating order and copolymer and homopolymer configurations with defects become predominant, even for the case of equal volume fractions. We have only presented results for the stoichiometric ratios $\alpha \leq 1$. However, "all situations" are accounted for as our model is symmetric with respect to the particle species.

Our theoretical results shed light on the experimental findings of oppositely charged comonomers that self-assemble into linear aggregates in aqueous solutions.[27,54] Especially, they rationalize the dependence of fraction of polymerized material in the saturation limit on the stoichiometric ratio. We find a very good agreement between our theoretical predictions and the experimental results. Even though our approach is restricted to nearest neighbor interactions, our model provides a good description of the experimental trends due to the strong negative coupling constant $J < -8.3$ and the strong self-screening of electrostatic interactions in alternating copolymers with complementary charges. Under these conditions, assemblies with nonperfect alternating order mainly comprise large blocks of alternating order and small blocks of ferromagnetic order. The assemblies can be regarded as alternating copolymers with defects where small blocks of the same species are bound together. For weaker negative coupling constants, the sections of alternating order become smaller relative to the sections of blocky order. Therefore, the electrostatic interactions on the assemblies will be

less screened and long-range interactions become important. Under such conditions, especially for stoichiometric ratios different from unity, restricting the electrostatic interactions to nearest-neighbor interactions is not accurate. An extension of our two-component model to an Ising model with longer range interactions is then required. Nonetheless, our results are relevant for the description of self-assembly behavior of any two-component system with strongly favorable interspecies binding as long as the interactions between the identical species are much weaker or repulsive. Other examples include chelating supramolecular polymers and chiral amplification in supramolecular polymers.

SUPPLEMENTARY MATERIAL

More details on the circular dichroism spectroscopy measurements characterizing the homopolymerization and copolymerization of glutamic acid and lysine derivatives are provided in the supplementary material. Additionally, a Python script for the numerical solution of the mass balance equations is included.

ACKNOWLEDGMENTS

R.V.B. and S.J.F. gratefully acknowledge the financial support from the German Research Foundation (http://www.dfg.de) within SFB TRR 146 (http://trr146.de). C. Berac is the recipient of a position through the DFG Excellence Initiative by the Graduate School Materials Science in Mainz (GSC 266).

NOMENCLATURE

b_{ij}	the magnitude of the bonded interaction free energies between two monomers of type $i \in \{A, B\}$ and $j \in \{A, B\}$, in units of the thermal energy k_BT
a_i	the activation free energy of species $i \in \{A, B\}$ in units of k_BT
Z_N	the partition function of an assembly of length N
$\rho(N)$	the number density of assemblies with the degree of polymerization N
$\overline{N}$	the number-averaged degree of polymerization including the monomers
$\overline{N}_p$	the number-averaged degree of polymerization excluding the monomers
$J \equiv \frac{1}{4}(b_{AA} - 2b_{AB} + b_{BB})$	the effective coupling constant in the Ising model
$H \equiv \frac{1}{2}[(b_{AA} - b_{BB}) + (\mu_A - \mu_B)]$	the magnetic field in the Ising model
$\bar{b} \equiv \frac{1}{4}(b_{AA} + b_{BB} + 2b_{AB})$	the average binding free energy
μ_i	the chemical potential of species $i \in \{A, B\}$
$\bar{\mu} \equiv 1/2(\mu_A + \mu_B)$	the average chemical potential
$\Delta\mu \equiv 1/2(\mu_A - \mu_B)$	the difference in chemical potentials
$\lambda_\pm$	the eigenvalues of a transfer matrix of the Ising model
$\Lambda_\pm \equiv \lambda_\pm \exp(\bar{b} + \bar{\mu})$	the effective fugacities of the bidisperse system
Φ_i	volume fraction of molecules of species $i \in \{A, B\}$
$\alpha = \Phi_A/\Phi_B$	the ratio of volume fraction of the two species, the so-called stoichiometric ratio
f	the mean fraction of polymerized material
f_i	the mean fraction of homopolymers composed of monomers of type $i \in \{A, B\}$
f_{AB}	the mean fraction of strictly alternating copolymers composed of equal concentration of A and B monomers
$\Phi_i^* = \exp(-b_i + a_i)$	the critical volume fraction associated with species i, demarcating the transition from minimal assembly to assembly predominated regime
$\Phi_{AB}^* = 2\exp(-b_{AB} + a)$	the critical volume fraction of alternating copolymers composed of equal concentrations of A and B species
$\Phi^*(\alpha)$	the critical volume fraction of a bidisperse system at stoichiometric ratio α
ϕ_i^m	the volume fraction of free monomers of species i
ξ_0	the correlation length of an antiferromagnetic chain in the limit $J \ll -1$
$f_{\text{alt}}(N)$	the fraction of copolymers of size N with perfect alternating order relative to all the assemblies of the same length
$f_{\text{B-homo}}(N)$	the fraction of homopolymers consisting of B species with size N relative to all the assemblies of the same length
$f_{\text{alt}}^{\text{tot}}$	the total fraction of alternating copolymers of any length
$f_{\text{B-homo}}^{\text{tot}}$	the total fraction of B-homopolymers of any length
q	the effective charge valency per monomer
b_{el}	the magnitude of electrostatic interactions between two neighboring charged monomers
$\lambda_B \equiv e^2/(4\pi\epsilon k_BT)$	the Bjerrum length in which e is the elementary charge and ϵ is the dielectric constant of the solvent

λ_D the Debye screening length
ℓ the average spatial distance between two monomers in a copolymer

APPENDIX: CALCULATIONS OF THE SPIN CORRELATION FUNCTION WITH OPEN BOUNDARY CONDITIONS

Here, we outline the calculation of the spin correlation function of the Ising model with open boundary conditions by means of the standard transfer matrix method. The partition function of Eq. (7) can be rewritten in terms of a transfer matrix W as

$$Z_N = \mathbf{e}^{E_0(N)} \sum_{S_1,S_N} \exp\left[\frac{H-\Delta b}{2} S_1\right] \prod_{i=1}^{N-1} \exp\left[J S_i S_{i+1} + \frac{H}{2}(S_i + S_{i+1})\right] \times \exp\left[\frac{H-\Delta b}{2} S_N\right] \tag{A1}$$

$$= \mathbf{e}^{E_0(N)} \mathbf{u} \mathrm{W}^{N-1} \mathbf{u}^{\mathrm{T}}, \tag{A2}$$

where $\Delta b \equiv 1/2(b_{AA} - b_{BB})$ and $\Delta\mu \equiv 1/2(\mu_A - \mu_B)$. The vectors $\mathbf{u} = (\exp[\Delta\mu/2] \exp[-\Delta\mu/2])$ and $\mathbf{u}^{\mathrm{T}}$ are associated with the free ends of the aggregates, and the transfer matrix is given by

$$\mathrm{W} = \begin{pmatrix} \mathbf{e}^{J+H} & \mathbf{e}^{-J} \\ \mathbf{e}^{-J} & \mathbf{e}^{J-H} \end{pmatrix}. \tag{A3}$$

We can diagonalize W using the rotation matrix[58]

$$\mathrm{P} = \begin{pmatrix} \cos\phi & -\sin\phi \\ \sin\phi & \cos\phi \end{pmatrix}, \tag{A4}$$

where ϕ satisfies

$$\cot(2\phi) = \exp(2J)\sinh(H), \quad 0 < \phi < \frac{\pi}{2}. \tag{A5}$$

The resulting diagonal matrix T reads

$$\mathrm{T} = \mathrm{P}^{-1}\mathrm{W}\mathrm{P} = \begin{pmatrix} \lambda_+ & 0 \\ 0 & \lambda_- \end{pmatrix}, \tag{A6}$$

where the eigenvalues $\lambda_\pm$ are given by Eq. (8). Therefore, the partition function yields

$$Z_N = \mathbf{e}^{E_0(N)} \mathbf{u} \mathrm{P} \mathrm{T}^{N-1} \mathrm{P}^{-1} \mathbf{u}^{\mathrm{T}}. \tag{A7}$$

The expectation value of a spin at site i to be in state S_i and a spin at site j to be in state S_j can be computed with respect to the partition function. Setting $1 \le i \le j \le N$ and expressing the spin matrix as[58]

$$\mathrm{C} = \begin{pmatrix} 1 & 0 \\ 0 & -1 \end{pmatrix}, \tag{A8}$$

the correlation function obeys[58]

$$\langle S_i S_j \rangle = Z_N^{-1} \mathbf{e}^{E_0(N)} \mathbf{u} \mathrm{W}^{i-1} \mathrm{C} \mathrm{W}^{j-i} \mathrm{C} \mathrm{W}^{N-j} \mathbf{u}^{\mathrm{T}}. \tag{A9}$$

Using the rotation matrix P, the rotated spin matrix R becomes

$$\mathrm{R} = \mathrm{P}^{-1}\mathrm{C}\mathrm{P} = \begin{pmatrix} \cos 2\phi & -\sin 2\phi \\ -\sin 2\phi & -\cos 2\phi \end{pmatrix}, \tag{A10}$$

which yields

$$\langle S_i S_j \rangle = Z_N^{-1} \mathbf{u} \mathrm{P} \mathrm{T}^{i-1} \mathrm{R} \mathrm{T}^{j-i} \mathrm{R} \mathrm{T}^{N-j} \mathrm{P}^{-1} \mathbf{u}^{\mathrm{T}}. \tag{A11}$$

Hence, the correlation function reduces to

$$\langle S_i S_j \rangle = \cos^2(2\phi) + \frac{x_+ \lambda_+^{N-1-j+i} \lambda_-^{j-i} + x_- \lambda_-^{N-1-j+i} \lambda_+^{j-i}}{x_+ \lambda_+^{N-1} + x_- \lambda_-^{N-1}} \sin^2(2\phi) + \frac{\lambda_+^{i-1}\lambda_-^{N-i} - \lambda_-^{i-1}\lambda_+^{N-i} + \lambda_-^{j-1}\lambda_+^{N-j} - \lambda_+^{j-1}\lambda_-^{N-j}}{x_+ \lambda_+^{N-1} + x_- \lambda_-^{N-1}} \times \sqrt{x_+ x_-} \cos(2\phi)\sin(2\phi). \tag{A12}$$

REFERENCES

[1] G. M. Whitesides and B. Grzybowski, Science **295**, 2418 (2002).
[2] H.-J. Schneider, *Supramolecular Systems in Biomedical Fields* (Royal Society of Chemistry, 2013), Vol. 13.
[3] M. Kirschner and T. Mitchison, Cell **45**, 329 (1986).
[4] J.-M. Lehn, Science **295**, 2400 (2002).
[5] P. J. Cragg, *Supramolecular Chemistry: From Biological Inspiration to Biomedical Applications* (Springer Science & Business Media, 2010).
[6] D. J. Rigden, *From Protein Structure to Function with Bioinformatics* (Springer, 2009).
[7] E. Buxbaum, *Fundamentals of Protein Structure and Function* (Springer, 2007), Vol. 31.
[8] A. Klug, Angew. Chem., Int. Ed. Engl. **22**, 565 (1983).
[9] J. K. M. Lehn and J. Sanders, Angew. Chem., Int. Ed. Engl. **34**, 2563 (1995).
[10] E. Krieg, M. M. Bastings, P. Besenius, and B. Rybtchinski, Chem. Rev. **116**, 2414 (2016).
[11] R. P. Sijbesma, F. H. Beijer, L. Brunsveld, B. J. B. Folmer, J. H. K. K. Hirschberg, R. F. M. Lange, J. K. L. Lowe, and E. W. Meijer, Science **278**, 1601 (1997).
[12] T. F. A. De Greef, M. M. J. Smulders, M. Wolffs, A. P. H. J. Schenning, R. P. Sijbesma, and E. W. Meijer, Chem. Rev. **109**, 5687 (2009).
[13] H. W. Binder, Monatsh. Chem.-Chem. Mon. **136**, 1 (2005).
[14] P. van der Schoot, Adv. Chem. Eng. **35**, 45 (2009).
[15] L. Brunsveld, B. Folmer, E. Meijer, and R. Sijbesma, Chem. Rev. **101**, 4071 (2001).
[16] R. Chakrabarty, P. S. Mukherjee, and P. J. Stang, Chem. Rev. **111**, 6810 (2011).
[17] R. Dobrawa and F. Würthner, J. Polym. Sci., Part A: Polym. Chem. **43**, 4981 (2005).
[18] D. Kushner, Bacteriol. Rev. **33**, 302 (1969).
[19] W. K. Kegel and P. van der Schoot, Biophys. J. **91**, 1501 (2006).
[20] M. F. Hagan, Adv. Chem. Phys. **155**, 1 (2014).
[21] R. F. Bruinsma, W. M. Gelbart, D. Reguera, J. Rudnick, and R. Zandi, Phys. Rev. Lett. **90**, 248101 (2003).
[22] C. E. Flynn, S.-W. Lee, B. R. Peelle, and A. M. Belcher, Acta Mater. **51**, 5867 (2003).
[23] C. F. Faul and M. Antonietti, Adv. Mater. **15**, 673 (2003).
[24] G. Tomba, M. Stengel, W.-D. Schneider, A. Baldereschi, and A. De Vita, ACS Nano **4**, 7545 (2010).
[25] H. Frisch, J. P. Unsleber, D. Lüdeker, M. Peterlechner, G. Brunklaus, M. Waller, and P. Besenius, Angew. Chem., Int. Ed. **52**, 10097 (2013).
[26] P. Ahlers, H. Frisch, and P. Besenius, Polym. Chem. **6**, 7245 (2015).
[27] P. Ahlers, K. Fischer, D. Spitzer, and P. Besenius, Macromolecules **50**, 7712 (2017).
[28] S. Jabbari-Farouji and P. van der Schoot, J. Chem. Phys. **137**, 064906 (2012).
[29] M. Cates and S. Candau, J. Phys.: Condens. Matter **2**, 6869 (1990).
[30] A. Ciferri, *Supramolecular Polymers* (CRC Press, 2005).
[31] G. Porte, J. Phys. Chem. **87**, 3541 (1983).

[32]A. V. Tobolsky and G. D. T. Owen, J. Polym. Sci. **59**, 329 (1962).
[33]J. van Gestel, P. van der Schoot, and M. A. J. Michels, Macromolecules **36**, 6668 (2003).
[34]L. Leibler and H. Benoit, Polymer **22**, 195 (1981).
[35]K. M. Hong and J. Noolandi, Polym. Commun. **25**, 265 (1984).
[36]S. T. Milner, T. A. Witten, and M. E. Cates, Macromolecules **22**, 853 (1989).
[37]C. Burger, W. Ruland, and A. N. Semenov, Macromolecules **23**, 3339 (1990).
[38]H. A. J. Markvoort, M. ten Eikelder, P. A. Hilbers, T. F. de Greef, and E. Meijer, Nat. Commun. **2**, 509 (2011).
[39]M. M. J. Smulders, M. M. L. Nieuwenhuizen, M. Grossman, I. A. W. Filot, C. C. Lee, T. F. A. de Greef, A. P. H. J. Schenning, A. R. A. Palmans, and E. W. Meijer, Macromolecules **44**, 6581 (2011).
[40]A. Das, G. Vantomme, A. J. Markvoort, H. M. M. ten Eikelder, M. Garcia-Iglesias, A. R. A. Palmans, and E. W. Meijer, J. Am. Chem. Soc. **139**, 7036 (2017).
[41]M. P. Evstigneev, Int. Rev. Phys. Chem. **33**, 229 (2014).
[42]B. Adelizzi, A. Aloi, A. J. Markvoort, H. M. Ten Eikelder, I. K. Voets, A. R. Palmans, and E. Meijer, J. Am. Chem. Soc. **140**, 7168 (2018).
[43]A. S. Buchelnikov, V. P. Evstigneev, and M. P. Evstigneev, Chem. Phys. **421**, 77 (2013).
[44]Y. Burak and R. R. Netz, J. Phys. Chem. B **108**, 4840 (2004).
[45]R. van Buel, "Supramolecular self-assembly of oppositely charged particles," M.S. thesis, Eindhoven University of Technology, 2016.
[46]N. Goldenfeld, *Lectures on Phase Transitions and Renormalization Group*, 1st ed. (Adison Wesley Publishing Company, 1992).
[47]P. van der Schoot, in *Supramolecular Polymers*, edited by A. Ciferri (CRC Press, 2005), Chap. 3.
[48]W. H. Carothers, Trans. Faraday Soc. **32**, 39 (1936).
[49]I. Nyrkova, A. Semenov, A. Aggeli, and N. Boden, Eur. Phys. J. B **17**, 481 (2000).
[50]E. Jones, T. Oliphant, P. Peterson *et al.*, SciPy: Open source scientific tools for Python, 2001.
[51]T. E. Oliphant, *A Guide to NumPy* (Trelgol Publishing, USA, 2006), Vol. 1.
[52]T. E. Oliphant, Comput. Sci. Eng. **9**, 10 (2007).
[53]S. Engel, D. Spitzer, L. Rodrigues, E.-C. Fritz, D. Strassburger, M. Schönhoff, B. Ravoo, and P. Besenius, Faraday Discuss. **204**, 53 (2017).
[54]H. Frisch, Y. Nie, S. Raunser, and P. Besenius, Chem.–Eur. J. **21**, 3304 (2015).
[55]P. Debye and E. Hückel, Phys. Z. **24**, 185 (1923).
[56]C. Schaefer, I. Voets, A. Palmans, E. Meijer, P. van der Schoot, and P. Besenius, ACS Macro Lett. **1**, 830 (2012).
[57]D. Spitzer, L. L. Rodrigues, D. Straßburger, M. Mezger, and P. Besenius, Angew. Chem., Int. Ed. **56**, 15461 (2017).
[58]R. J. Baxter, *Exactly Solved Models in Statistical Mechanics* (Academic Press, 1982).